Introduction to Bragg Diffraction Imaging ("X-ray Topography")

José Baruchel

baruchel@esrf.fr

Outline

- Introduction
- Basic contrast mechanisms
- Diffraction topographic techniques
- Simulations of topographic images
- Combination of techniques (RCI, topo-tomography)
- Bragg diffraction imaging at modern SR facilities

- **Introduction**

⇨ Bragg diffraction imaging (X-ray topography)

⇨ what can we see on a topograph

⇨ Order of magnitude of the distortions

⇨ How the technique developed

- Basic contrast mechanisms
- Diffraction topographic techniques (overview)
- Simulations of topographic images
- Combination of techniques (RCI, topo-tomography)
- Conclusion: new possibilities of modern synchrotrons for Bragg diffraction imaging

Bragg diffraction imaging ("topography")

basic principle for an extended, homogeneous, white or monochromatic beam

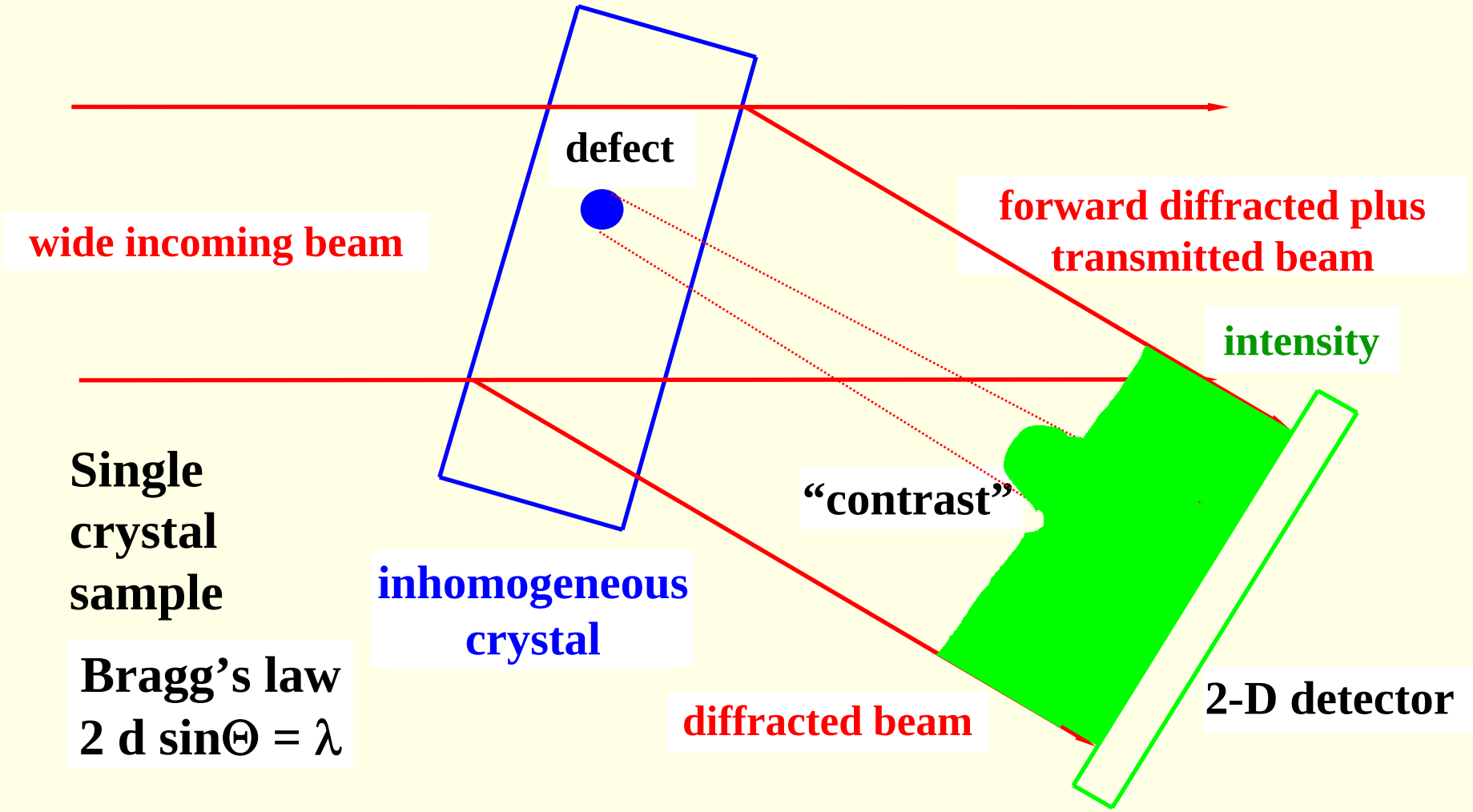

What can we see on a topograph?

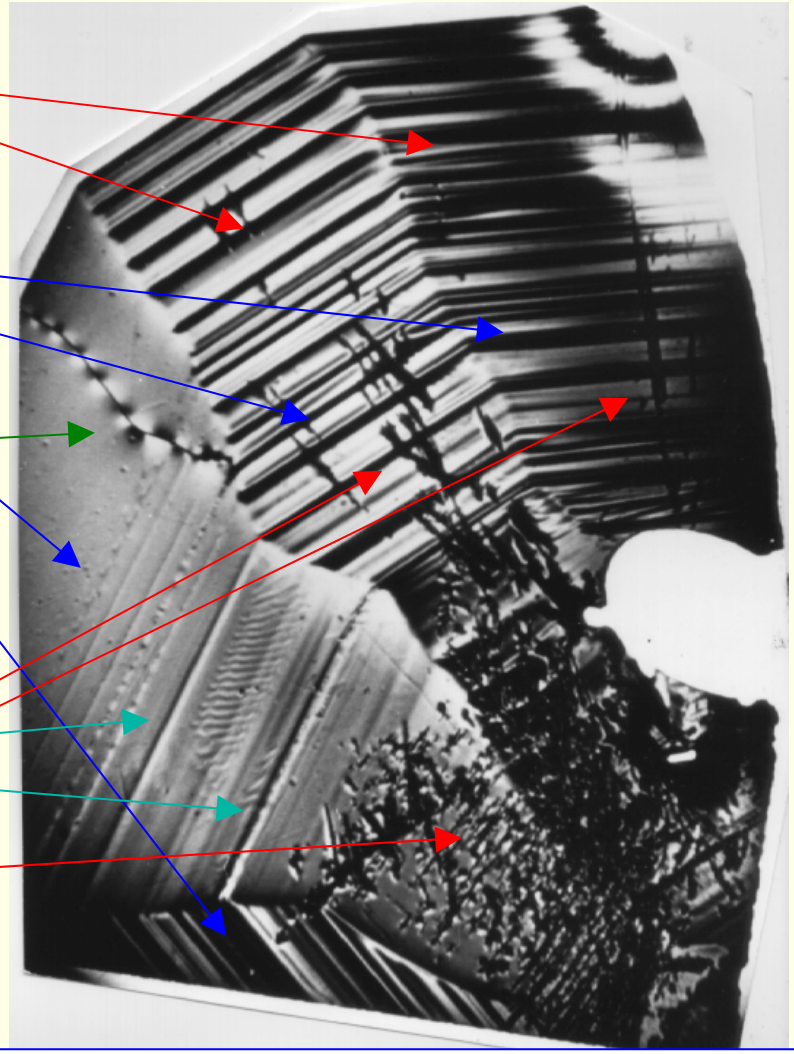

Transmission X-ray topograph of a flux grown Ga-YIG ($Y_3Fe_{5-x}Ga_xO_{12}$, x ≈1) crystal plate, $MoK_{\alpha 1}$-radiation (λ=0.709 Å), 44-4 reflection

What else do we see within a Bragg spot?

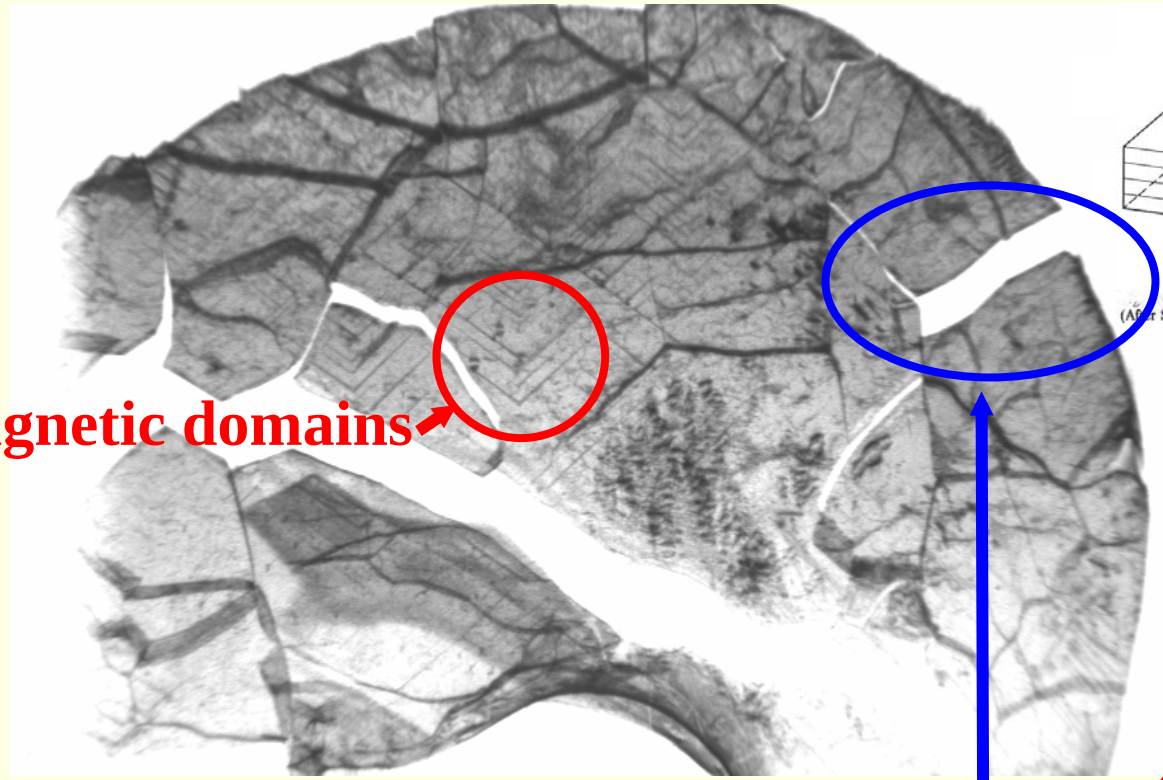

magnetic domains

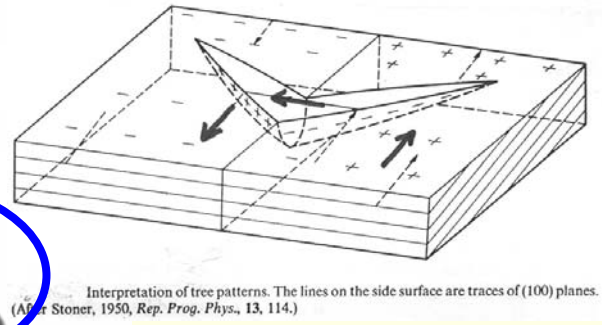

Interpretation of tree patterns. The lines on the side surface are traces of (100) planes.
(After Stoner, 1950, *Rep. Prog. Phys.*, 13, 114.)

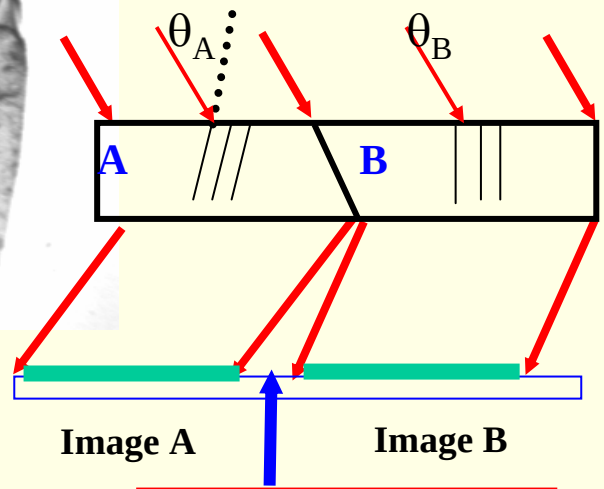

Subgrain boundary

Gap between the two images

« Section » topography

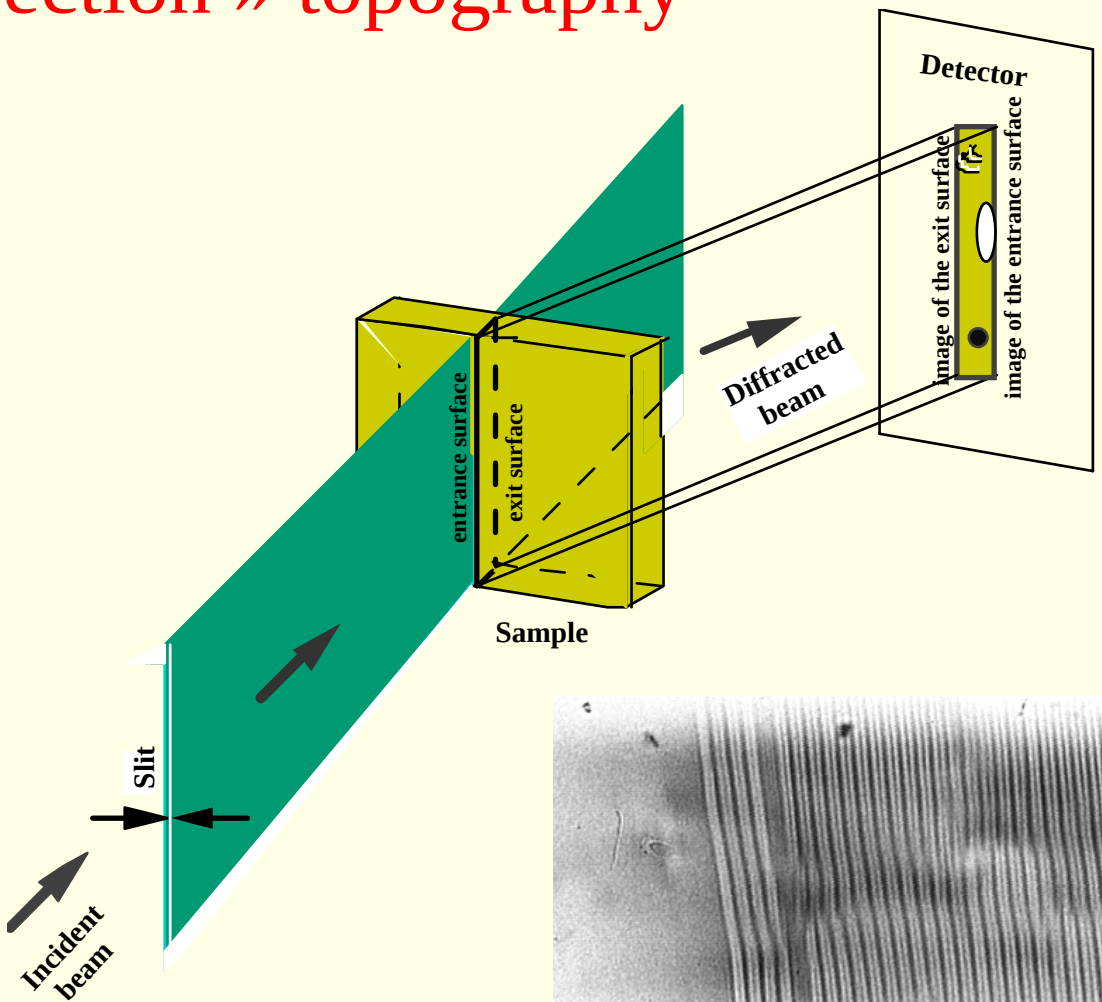

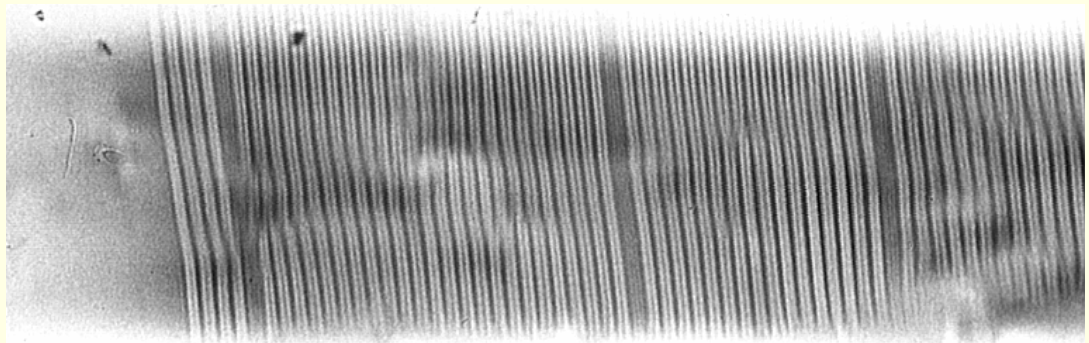

(rotated by 90° with respect to the drawing)

Order of magnitude of the distortions observed on the previous topographs

(either $\delta\theta$, or Δd, or combination of both)

Growth striations	$\#10^{-4}$
magnetic domains (magnetostriction)	$\#10^{-6}$
misorientation between subgrains	$\#10^{-4}$ -10^{-3}
dislocations	function of the distance to the core; related to the width of the image

Main features (and limits) of the technique

Spatial resolution: $\approx 1\mu m$

Strains possible to detect: up to 10^{-8}

Sample dimensions:

laterally: from $\sim 50\mu m$ ($\Leftrightarrow$ resolution!)
to centimeters and decimeters

thickness: $\sim 1\mu m$ - 10 mm

Image formation: defects are imaged
through their associated long-range distortion field

How the technique developed?

need to characterize large crystals for microelectronics industry

typical exposure times: 2-20 hours

Early days of high-resolution x-ray topography

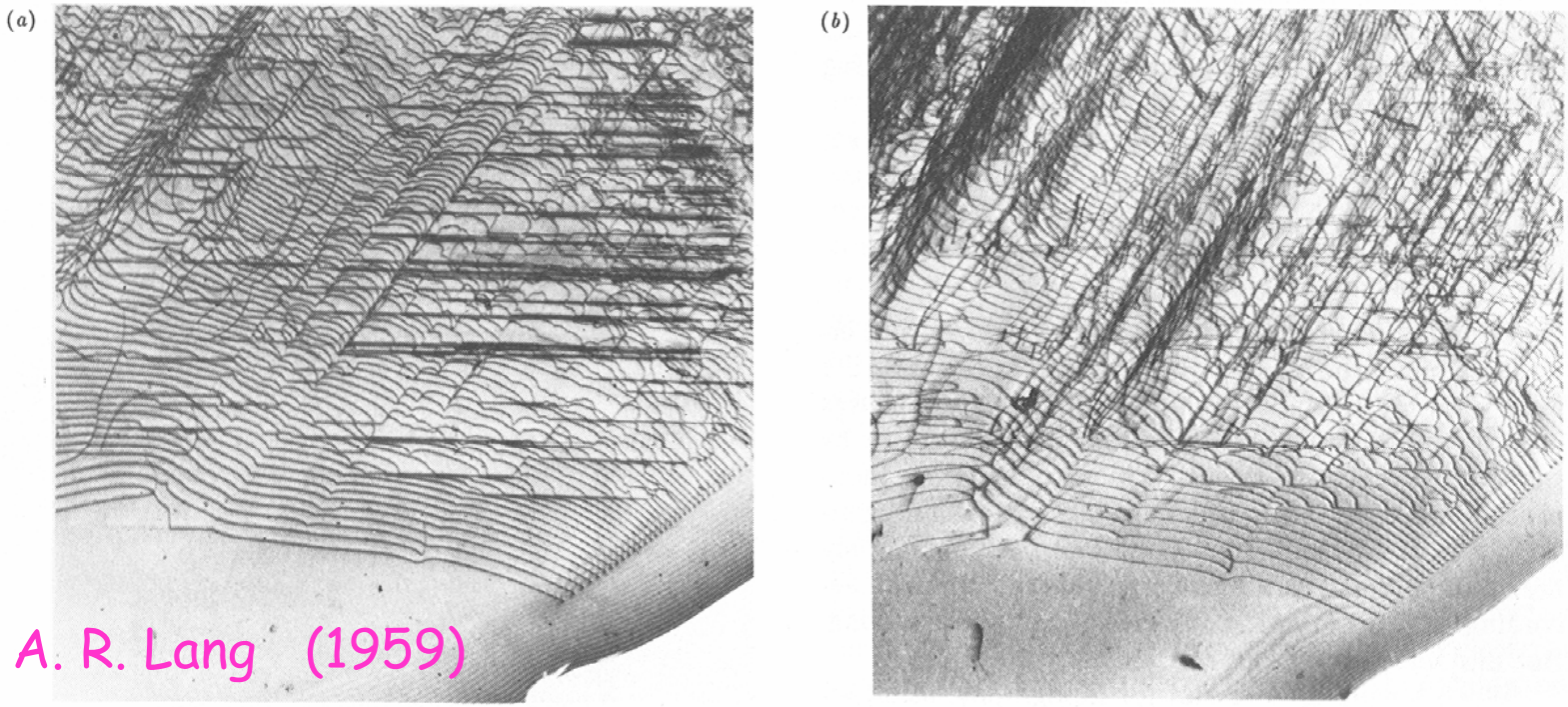

Figure 4. Projection topographs of part of $(11\bar{1})$ slice of silicon 1 mm thick, direction $[\bar{1}10]$ horizontal. Field width 6.25 mm. Radiation AgKα_1. Diffraction vector directions shown in figure 5. Reflections: (*a*) $\bar{1}\bar{1}\bar{1}$; (*b*) $\bar{2}20$; (*c*) $1\bar{1}1$; (*d*) $1\bar{3}1$.

ID19, ESRF “parallel beam imaging” BL exposure times: 0.01-100 s

- Introduction
- **Basic contrast mechanisms**

⇨ Some dynamical theory results

⇨ Effects of inhomogeneities

- Structure factor contrast
- Orientation contrast
- “Extinction” contrast

⇨ More on topographic images

- Diffraction topographic techniques (overview)
- Simulations of topographic images
- Combination of techniques (RCI, topo-tomography)
- Bragg diffraction imaging at modern synchrotrons

Some results of dynamical theory

necessary to understand the contrast mechanisms

(restricting to symmetrical transmission geometry -Laue case-)

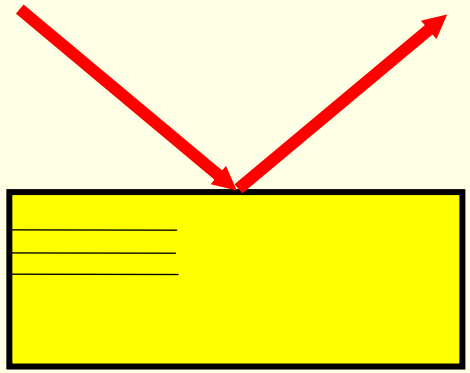

“Bragg” or reflection case

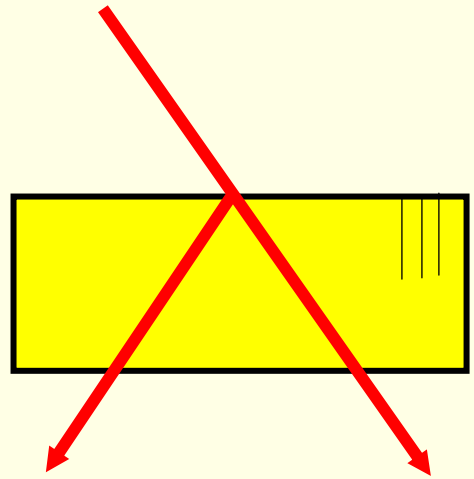

“Laue” or transmission case

Bragg diffraction in a perfect crystal

- Bragg's law $2d \sin\theta = \lambda$

- for a monochromatic plane wave, the diffraction condition should therefore be a δ function: not very "physical"

- The dynamical theory of diffraction tell us that the actual diffraction condition is such that wavefields propagate in the crystal if the incident beam propagation vector lies within w_h^{θ} around the « exact Bragg position »

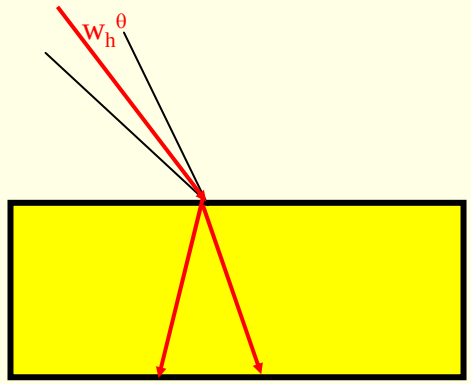

Plane wave beam: Darwin width

Symmetrical Laue case

$$w_h^{\theta} = \frac{2\lambda^2 C_p |F_h| r_0}{\pi V_C \sin 2\theta_B}$$

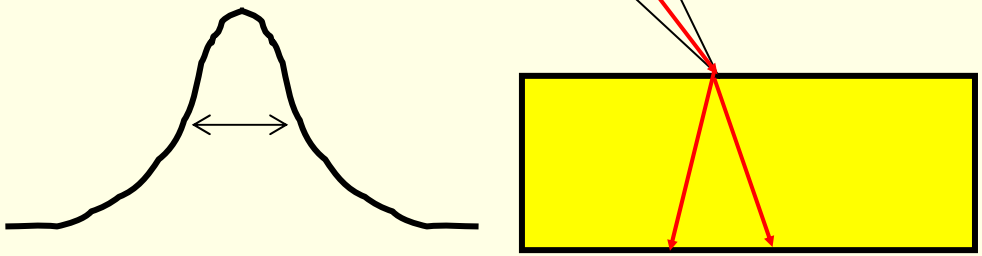

w_h^{θ} intrinsic width of the diffraction curve (Darwin width)

➔ typical values # 10^{-5}-10^{-6} radians

C_p: polarization factor V_C : unit cell volume F_h : structure factor

r_o is the classical radius of the electron

Extinction (or Pendellösung) length

The wavefields propagate and interfere within the whole "Borrmann" fan ABC

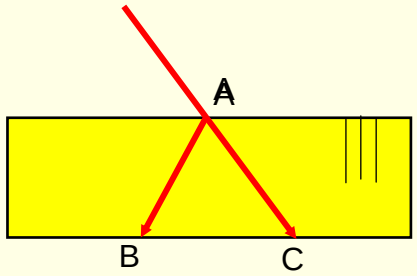

Characteristic coupling length between wavefields Λ_h: extinction length

$$\Lambda_h = (\pi V_c \cos\theta_B) / (\lambda C_p |F_h| r_0)$$

➔ typical values 1 to 100 μm

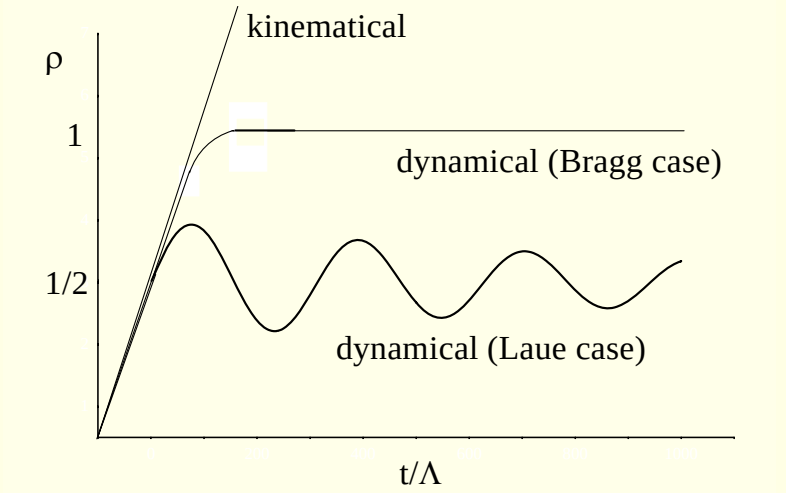

Integrated reflectivity ρ, non-absorbing perfect crystal

(Laue" and "Bragg" cases, as a function of reduced thickness t / Λ_h)

Equal thickness fringes

Wedge shaped crystal

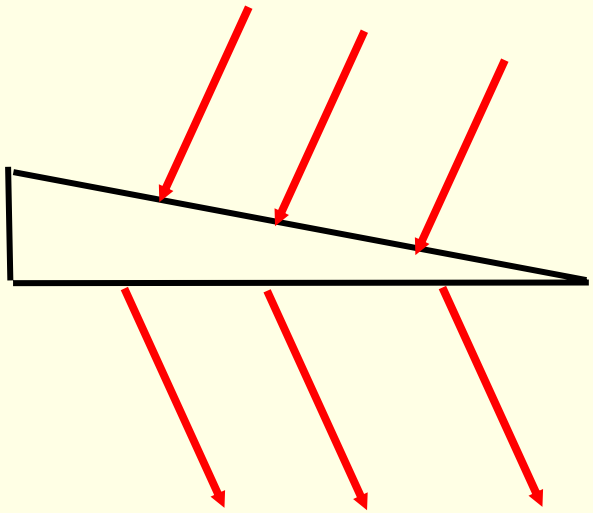

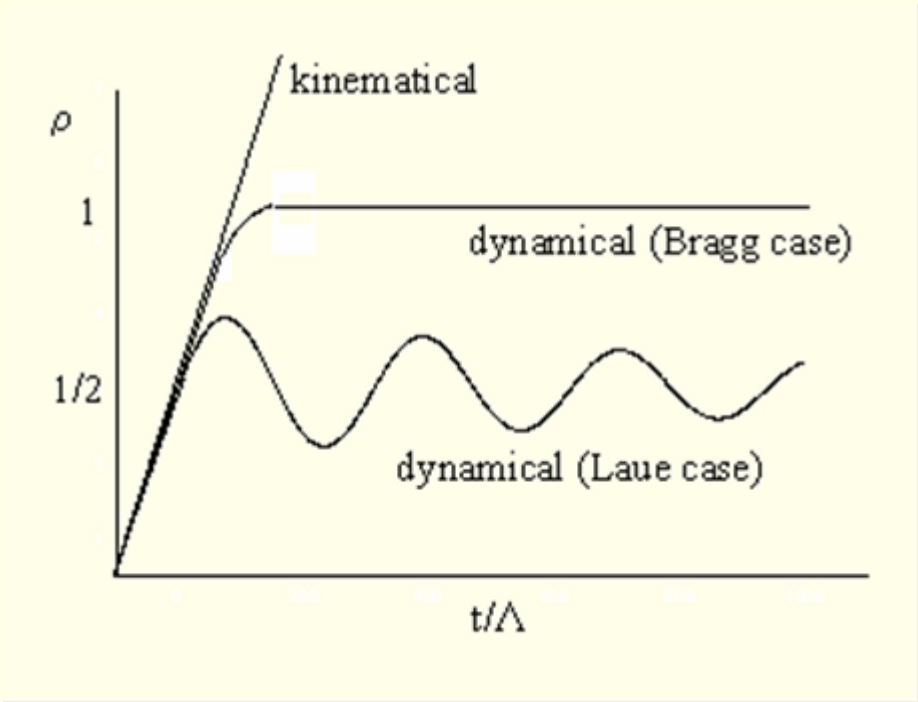

Contrast that corresponds to a dynamical theory effect

Effect of imperfections: contrast mechanisms (1)

Non-absorbing plate-shaped crystal illuminated by a parallel and polychromatic beam

➔ the direction and intensity of the locally diffracted intensity depends upon

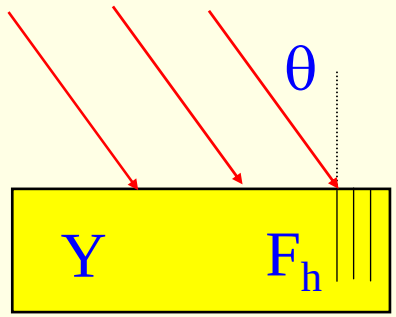

➔ θ, angle formed by the lattice planes and the beam

➔ F_h , structure factor

➔ Y, "extinction parameter" (which is intended to incorporate all the modifications introduced by the crystal inhomogeneities on the dynamical theory results)

Effect of imperfections: contrast mechanisms (2)

The beams diffracted by two neighbouring regions A and B of the sample produce contrast on the topograph if

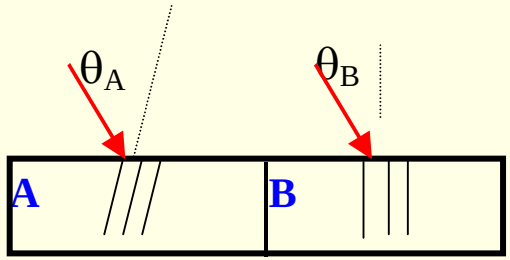

1) θ_A & θ_B different (regions A and B are misoriented) **orientation contrast**

2) $(F_h)_A$ & $(F_h)_B$ different (modulus or phase) **structure factor contrast**

3) Y_A & Y_B different, the two regions display **extinction contrast**

Orientation Contrast

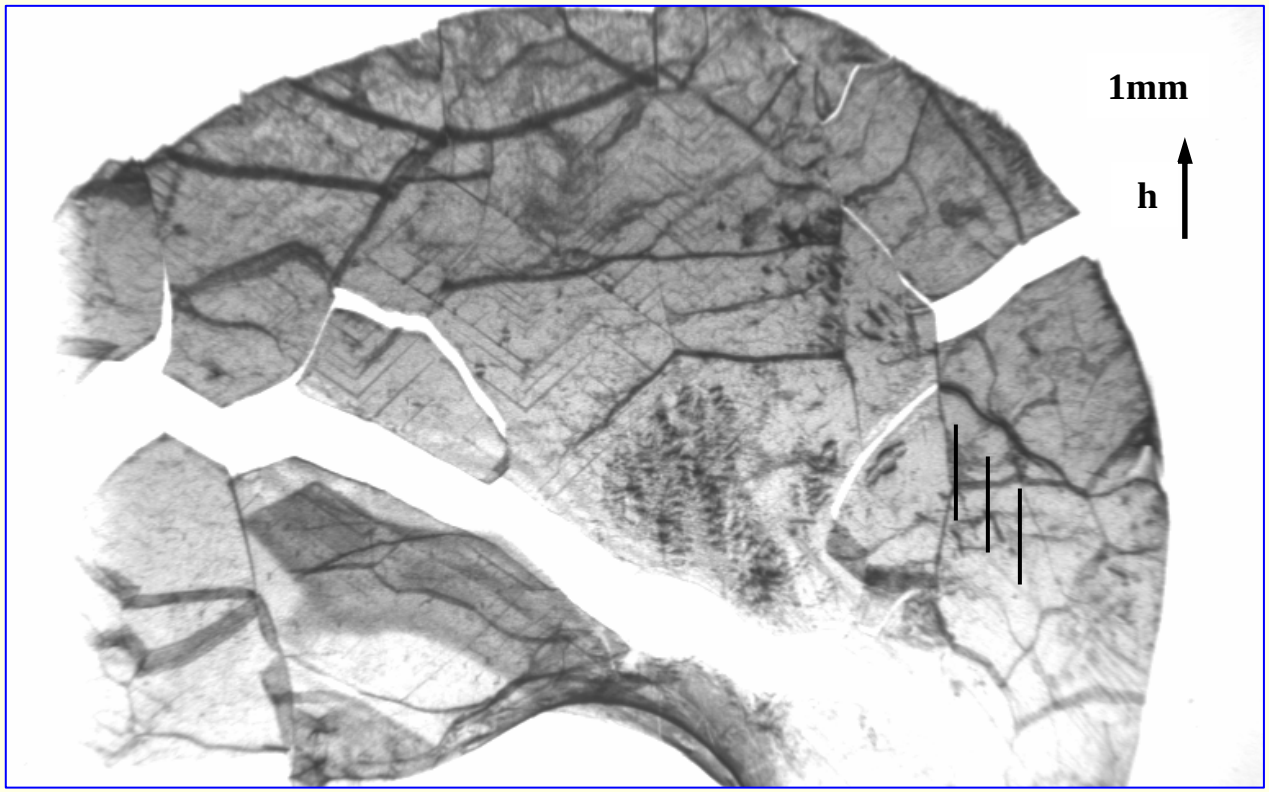

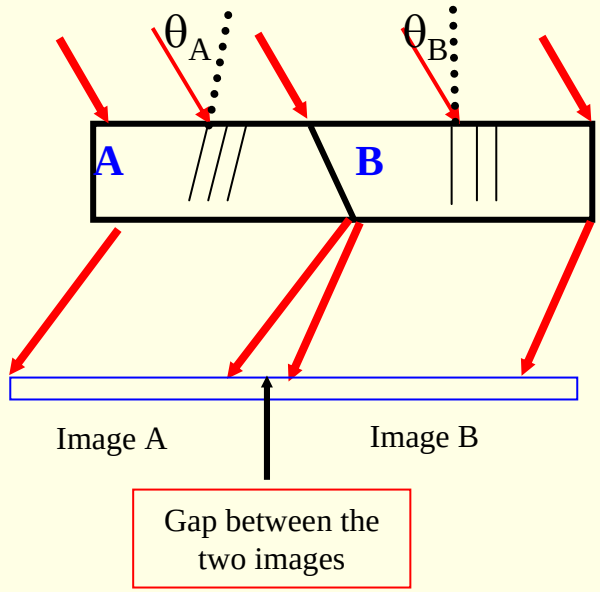

Structure factor contrast (amplitude)

Quartz - twins with (hki±l)

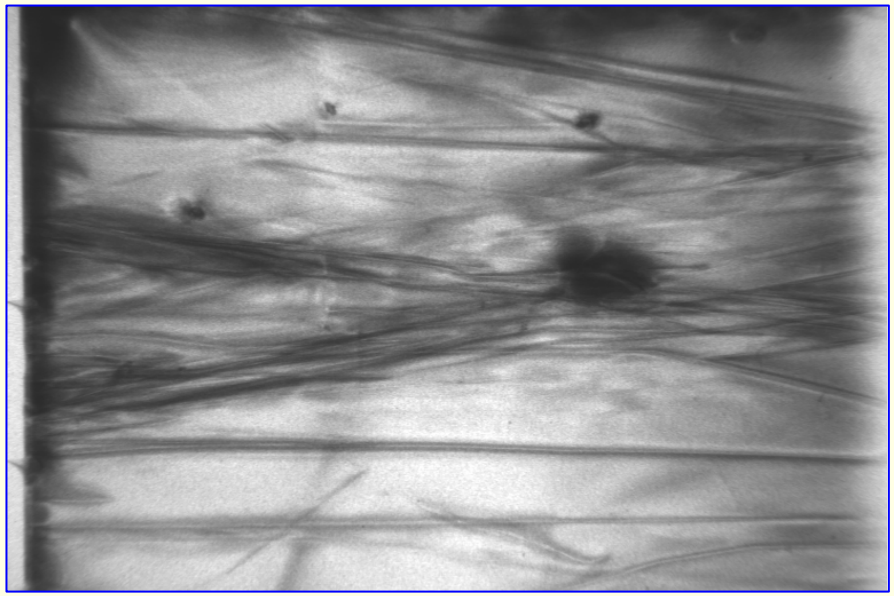

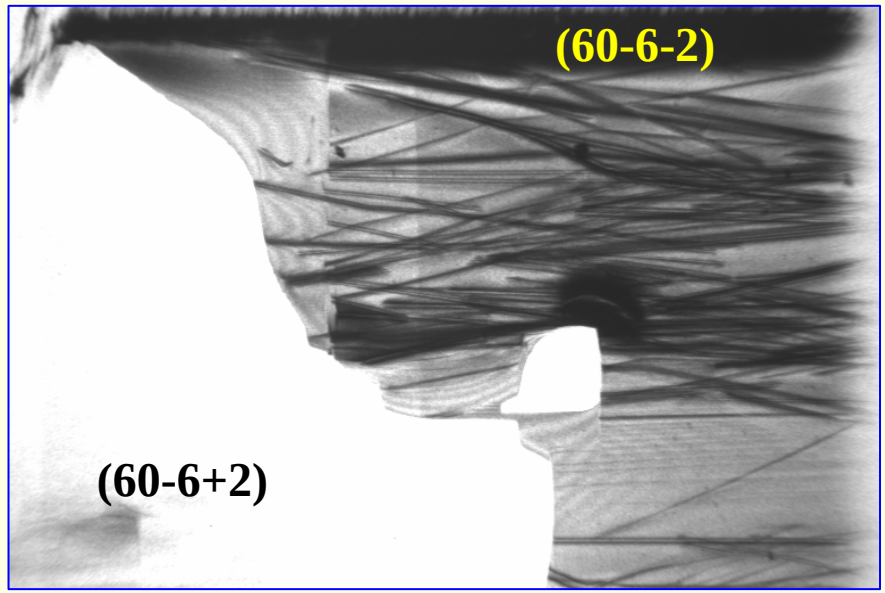

h

(0006)

2 mm

h

(60-6±2)

$F_{60\text{-}6\text{-}2} = 21 \quad F_{60\text{-}6+2} = 2$

BRAGG DIFFRACTION

Diffracted wave is proportional to the structure factor F(h)

$$F(h)=\sum_{j}^{cell} f_j e^{-2\pi i h x_j}$$

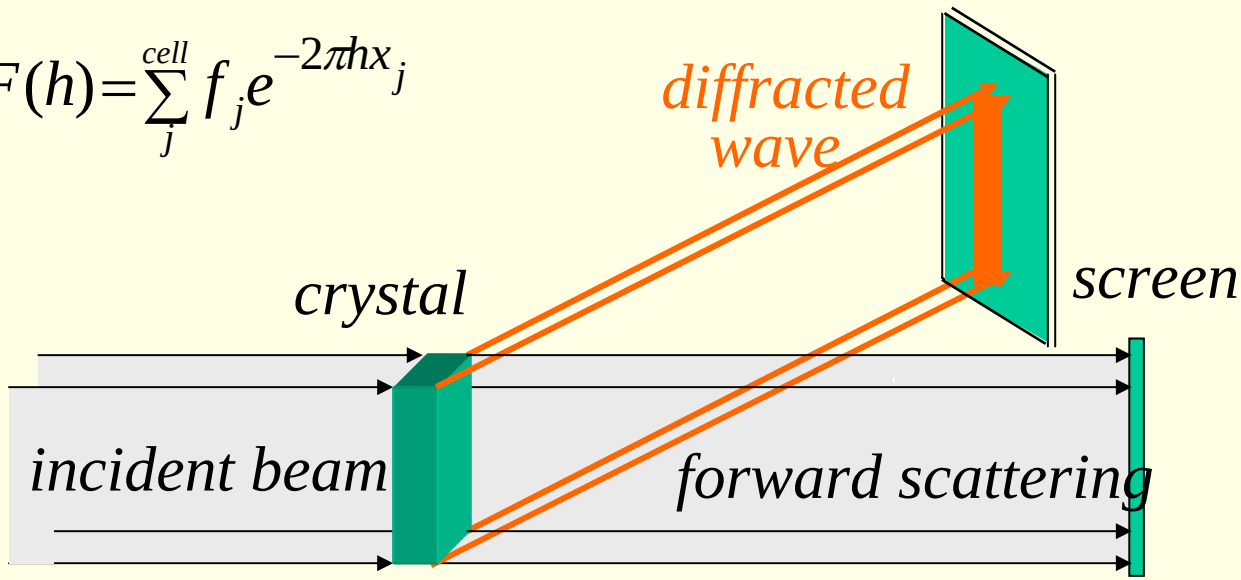

Structure factor contrast (phase)

When working with a ***coherent*** X-ray beam, and if the phases of the structure factors are different (ϕ_A different from ϕ_B) as can be the case for **ferroelectric domains**, Bragg and Fresnel diffraction can be combined to reveal the domains

domain I: $F_{hk\ell}$

domain II: $F_{-h-k-\ell}$

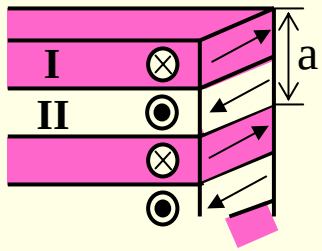

$$|F_{hk\ell}| \sim |F_{-h-k-\ell}|$$

but $\varphi_I \neq \varphi_{II}$

phase shift $\Delta\varphi = \varphi_I - \varphi_{II}$

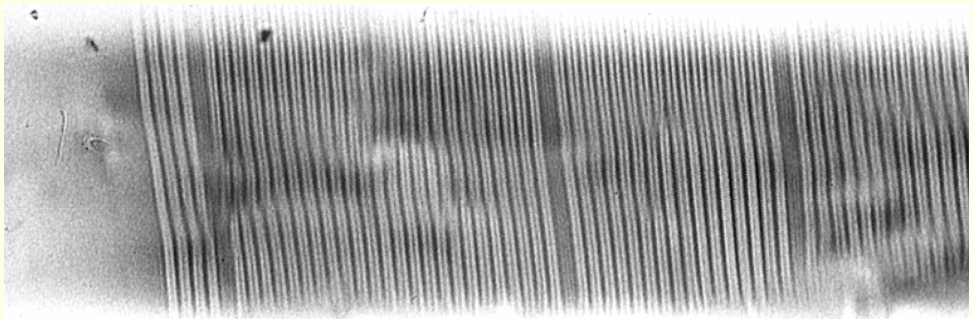

Section topograph in transmission mode
KTP, period of poling 9μm
Distance crystal-detector = 40 cm

POSSIBLE ORIGINS OF A PHASE SHIFT IN BRAGG DIFFRACTED WAVE

wave emerging from the crystal: phase modulations φ(x) can be produced by regions (I, II) with different:

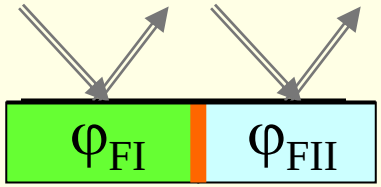

- structure factor phases φ_F: $F=|F|\, e^{i\varphi_F(x)}$

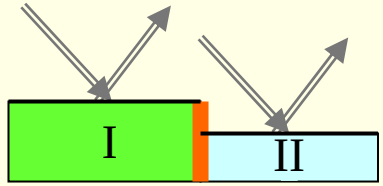

- surface profiles (e.g. steps) φ_{step}

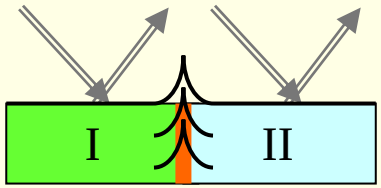

- distortions of reflecting planes φ_α

- distance between regions ℓ different from ℓ = n×cell parameter

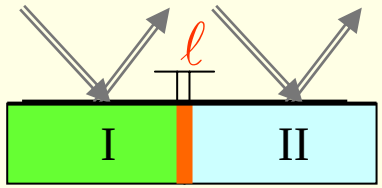

- ...

Effective misorientation

- image of defect produced by regions which are distant (μm range) from defect core
- this distance depends not only on the defect, but also on the diffraction process itself
- the lattice distortion acts on diffraction through the effective misorientation δθ

$$\delta\theta = -(\lambda / \sin 2\theta_B)\, \partial(\mathbf{h}\cdot\mathbf{u})/\partial s_h$$

δθ = 0 if **u** perpendicular to **h**: defect not visible on the topograph

Example: dislocation not visible

when **h.b** = 0,

(b being the Burgers vector -arrow-)

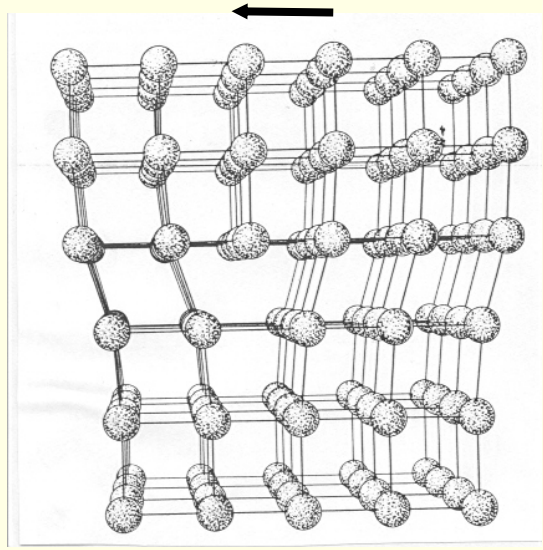

Example: white beam topography of GaAs

Vertical Gradient Freeze technique

B. Birkmann/Erlangen

White beam topography

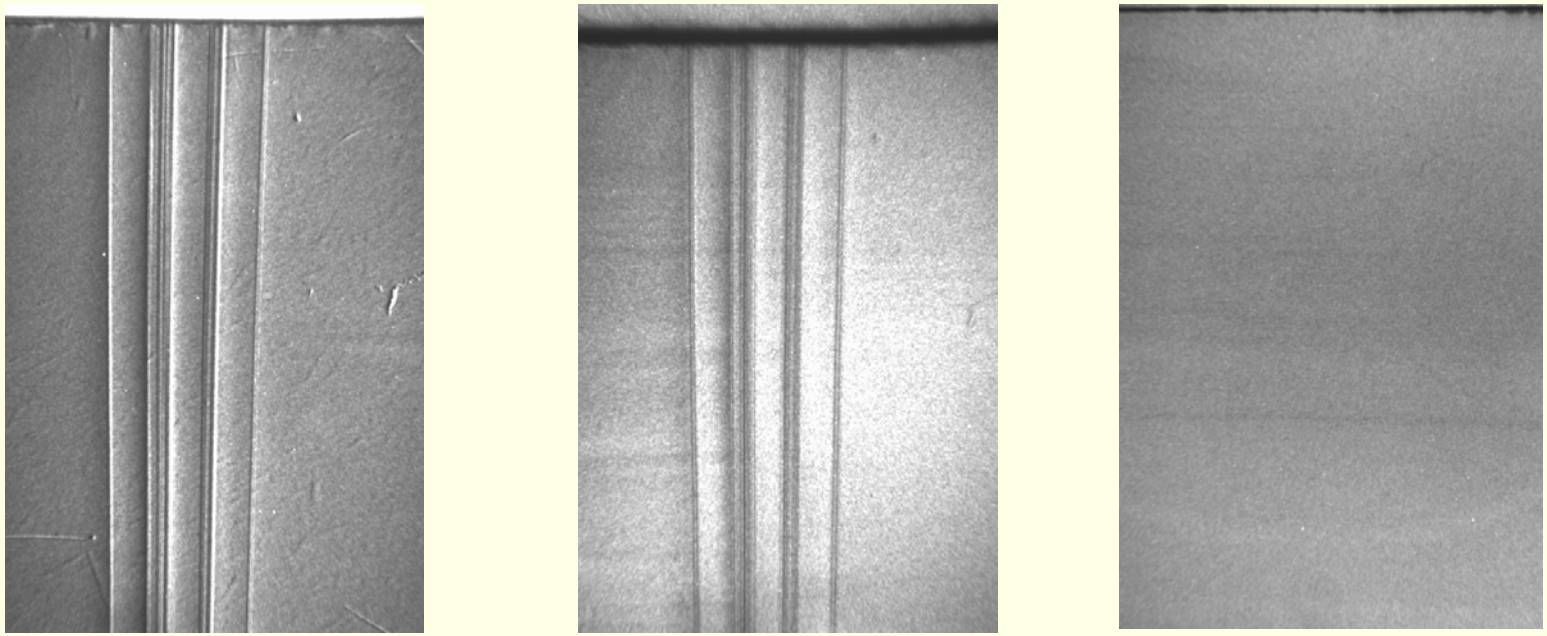

Contrast extinction for b ⊥ h ➡ Edge dislocation with b || [2-20]

Precipitate in GaAs

White beam topography

Sample grown by the Vertical Gradient Freeze technique

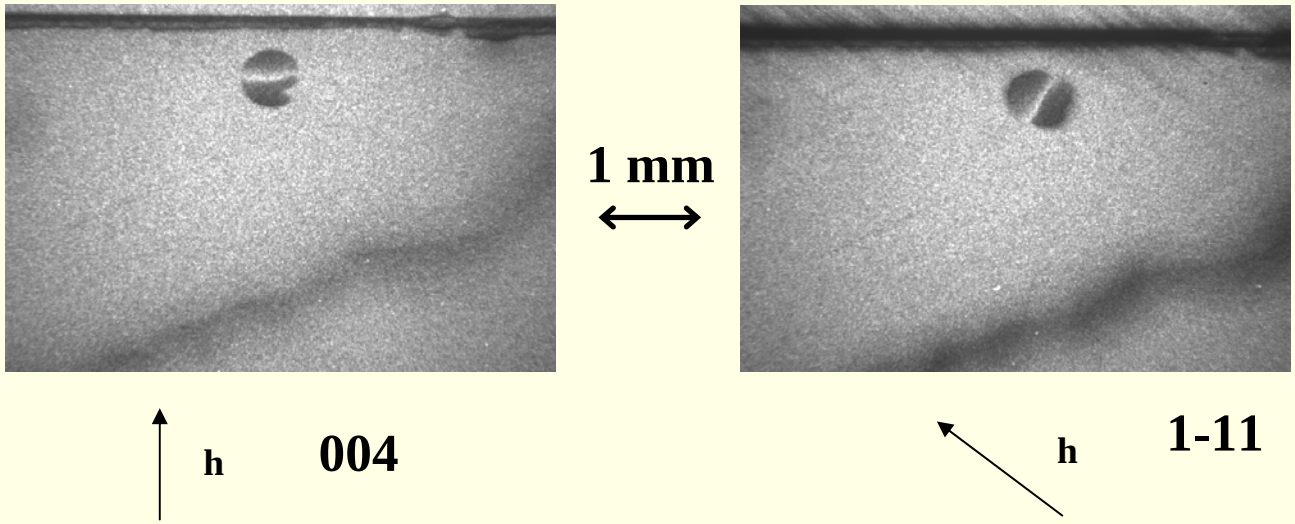

$\mathbf{u} = A \cdot \mathbf{r} / r^3$ $\mathbf{u} \cdot \mathbf{h} = 0$ ➔ Line out of contrast: $\mathbf{u} \perp \mathbf{h}$

Direct, or « extinction », image

➔ polychromatic, parallel, beam on a crystal

➔ Defect (inclusion, dislocation,...) ➔ distortion field in volume V

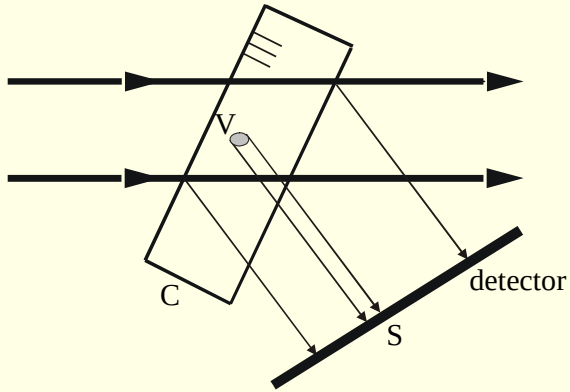

➔ a wavelength range $\Delta\lambda/\lambda = w_h^{\theta} / (\mathrm{tg}\ \theta_B)$ ($\sim 10^{-4}$) participates in diffraction by the "perfect" matrix crystal (where w_h^{θ} is the Darwin width and θ_B is the Bragg angle)

➔ regions around the defect are in Bragg position for components of the incoming beam which are outside this spectral range

➔ the defect thus leads to **additional diffracted intensity** on the detector

Width of the image of a defect

effective misorientation $\delta\theta$

$\delta\theta = - (\lambda / \sin 2\theta_B)\, \partial(\mathbf{h}\cdot\mathbf{u})/\partial s_h$

Darwin width w_h^{θ}

$w_h^{\theta} = (2\lambda^2 C_p |F_h| r_0) / (\pi V_c \sin 2\theta_B)$

Width of the direct image corresponds to the contribution of regions such that $\delta\theta$ is of the order of w_h^{θ}.

larger width if w_h^{θ} decreases
(i.e. if λ or F_h decrease)

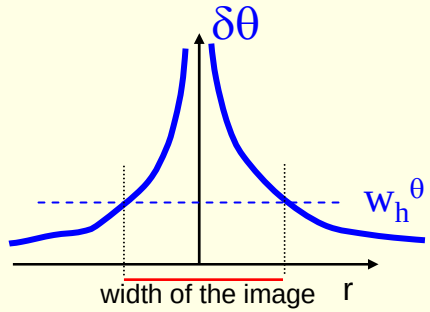

➔ "intrinsic" image widths 1-100 μm

Absorbing crystals

➔ When taking absorption into account, the situation can change drastically.

➔ Direct images do not occur in the high absorption case, and are replaced by dips in the intensity (disruption of the anomalous transmission or Borrmann effect).

➔ Both types of images (“additional” intensity and “dips”) are simultaneously present on the topographs, as well as interference fringes (“dynamical” images) for samples with intermediate absorption ($\mu t \sim 2\text{-}4$).

Example of low and high absorption topographs

precipitates in Cz-Si

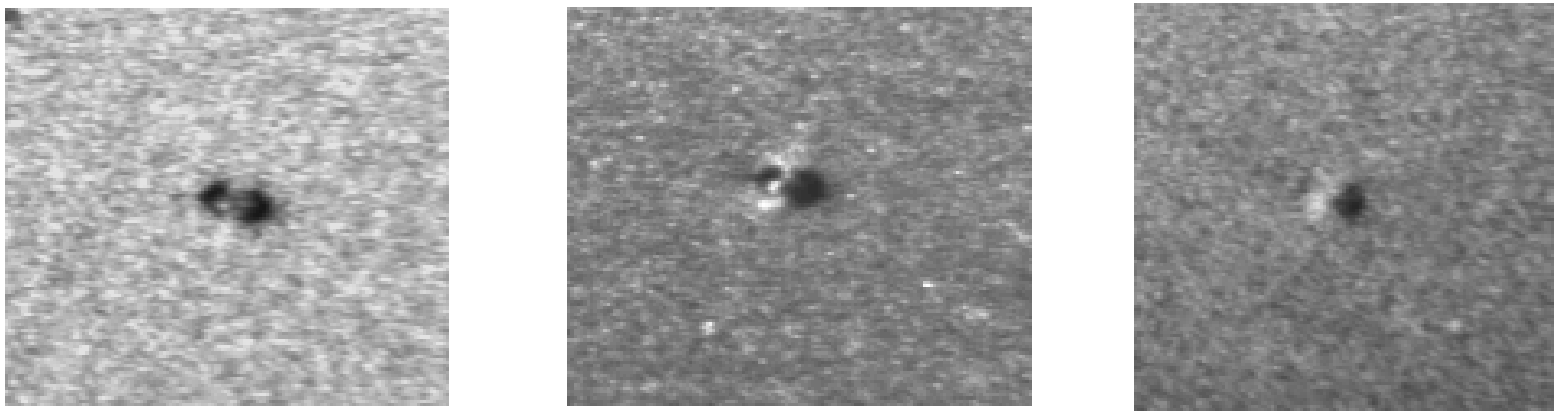

Image evolves, with increasing absorption, from black to black-white and even (for μt>10) to completely white

Contrast asymmetries due to absorption

Precipitate in GaAs

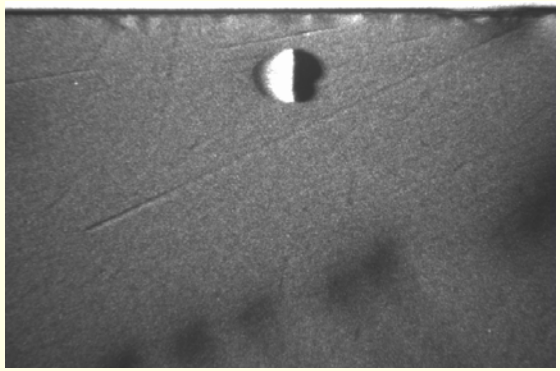

2-20 - reflection

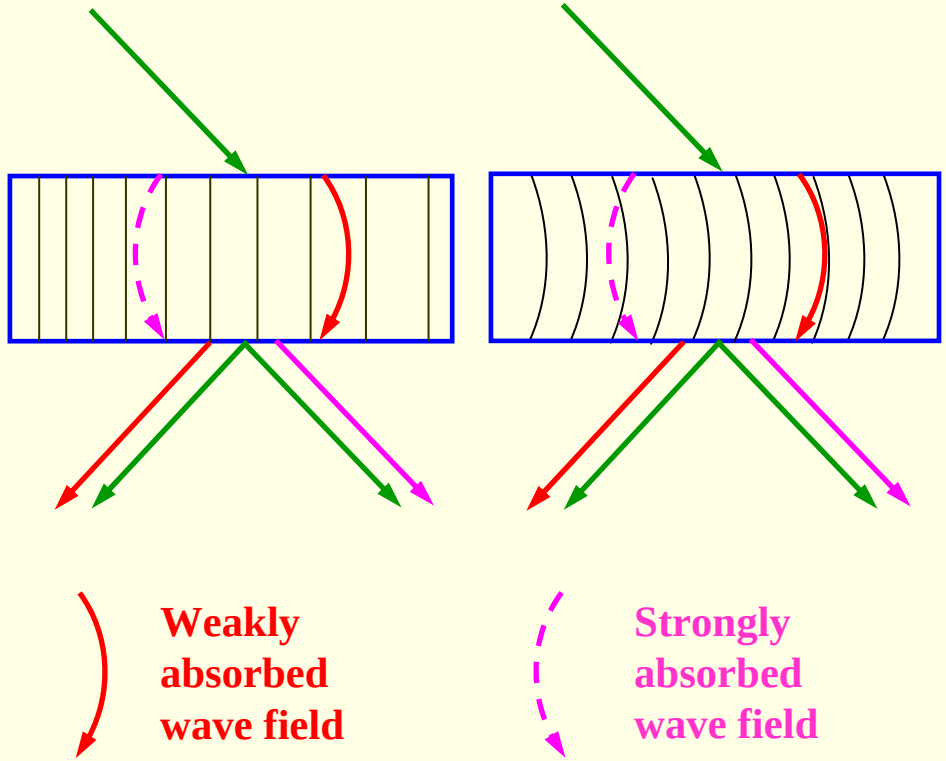

Enhanced contribution in k_h-direction
enhanced intensity I_h

- Introduction
- Basic contrast mechanisms
- **Diffraction topographic techniques**

  ⇨ white or monochromatic, integrated or plane wave

  ⇨ Extended and restricted beam

  ⇨“weak beam”
- Simulations of topographic images
- Combination of techniques (RCI, topo-tomography)
- Bragg diffraction imaging at modern synchrotrons

"White Beam Topography" is the simplest SR-based topographic technique

Usual setup for Laue technique, but incoming "white" beam is

⇨ **wide, illuminates all or a substantial fraction of the sample**

⇨ **low divergence , small angular size of the source seen from the sample**

Laue imaging ("white beam topography")

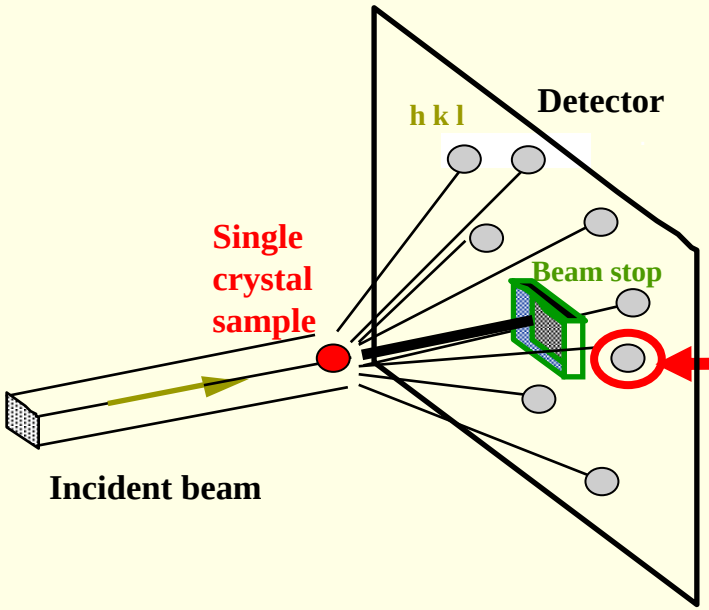

each Laue spot is a Bragg diffraction image that allows observing, when looking inside the spot, inhomogeneities like defects, domains, phases…

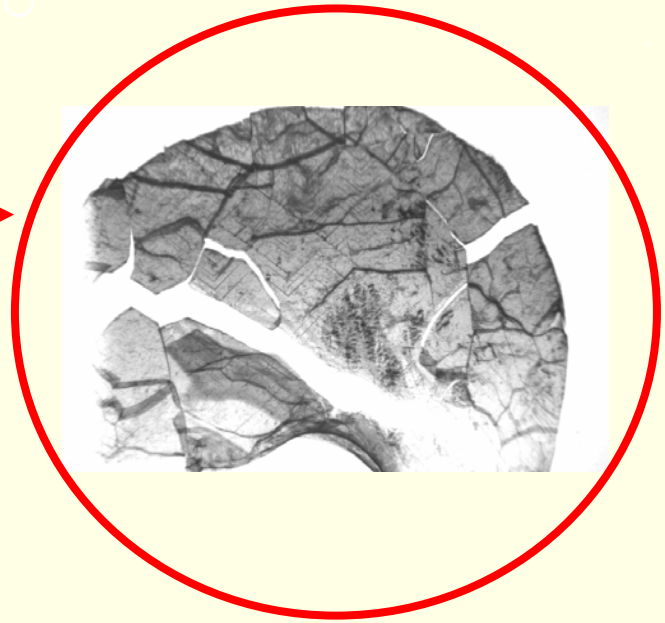

Crystallization of metallic alloys (liquid-solid transition)

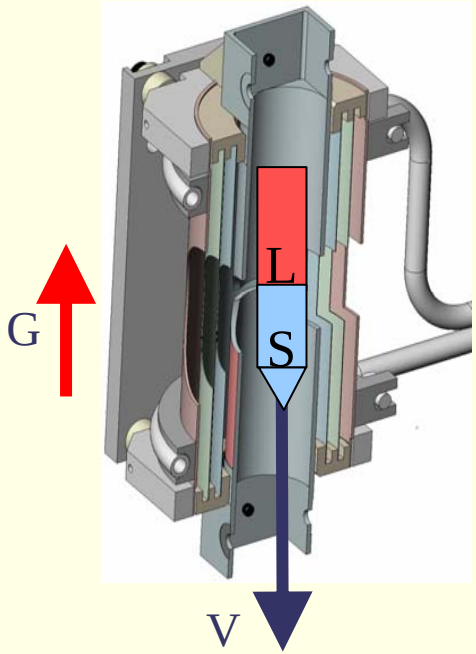

Bridgman furnace with two independent heating elements

The white beam is important because the orientation of the growing crystal is not known in advance

Bragg images recorded during the solification of a binary alloy

increasing the growth velocity ⇨ plane to cellular instability

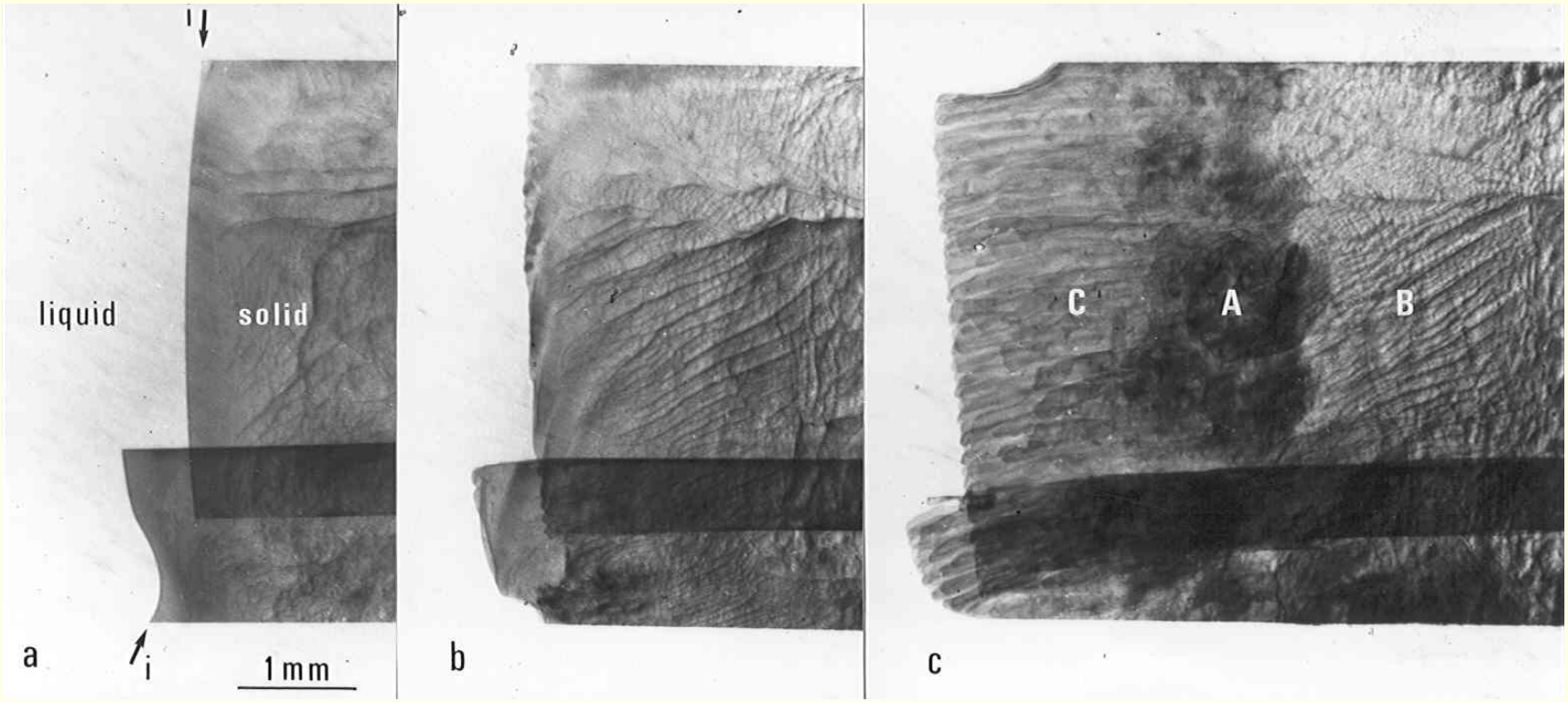

Jourdan, Grange, Gastaldi

White beam topography (transmission geometry)

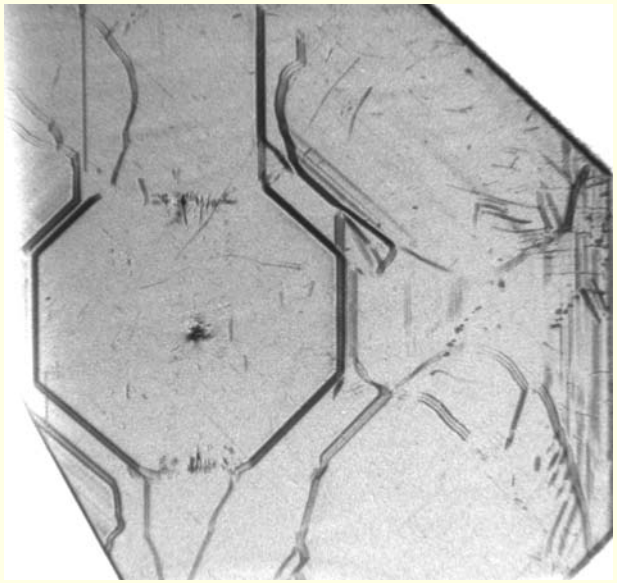

[2$\bar{2}$0]

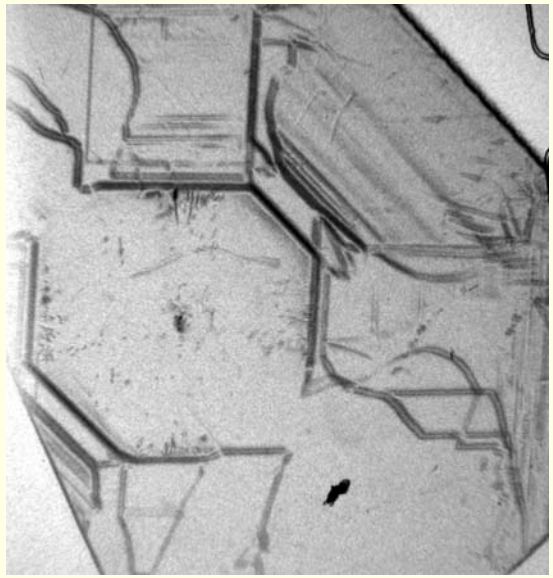

[400]

2 mm

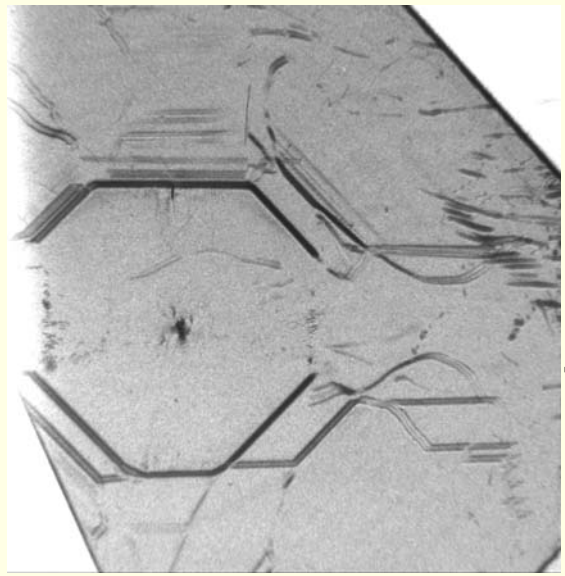

[220]

(001) Ib diamond

Simple set-up

- **no sample orientation necessary**
- **simultaneous reflections (extinction of contrast)**
- **all crystal parts (also misoriented ones) visible simultaneously**

White beam topography

⇨ **sensitive only to lattice plane inclination**

(misorientation contrast)

⇨ **limited sensitivity to weak distortions (~10^{-6})**

⇨ **quantitative analysis complicated**

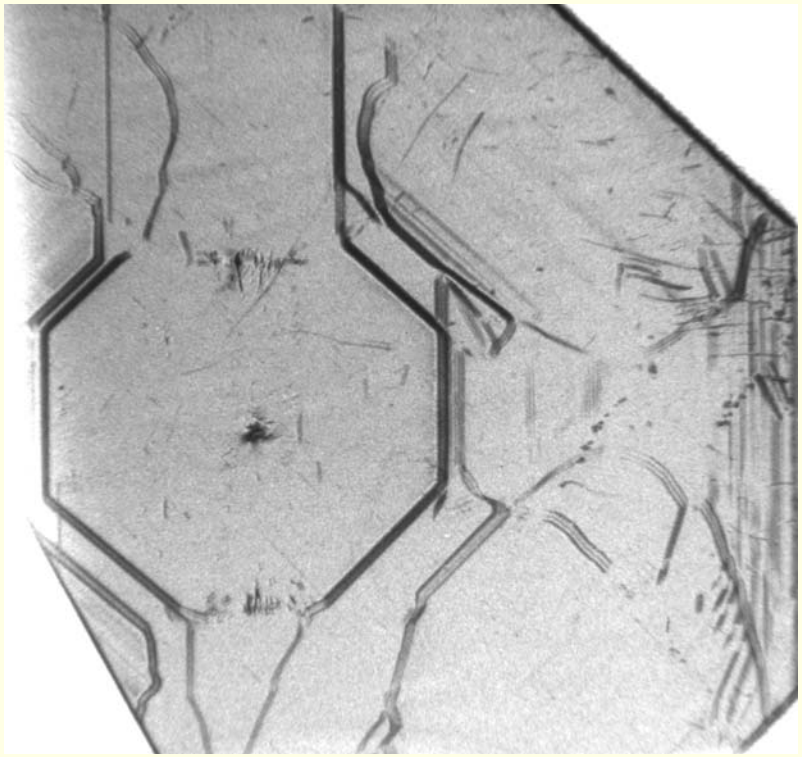

Double crystal topography (reflection geometry)

« integrated » image

« non-integrated » image

White beam topography

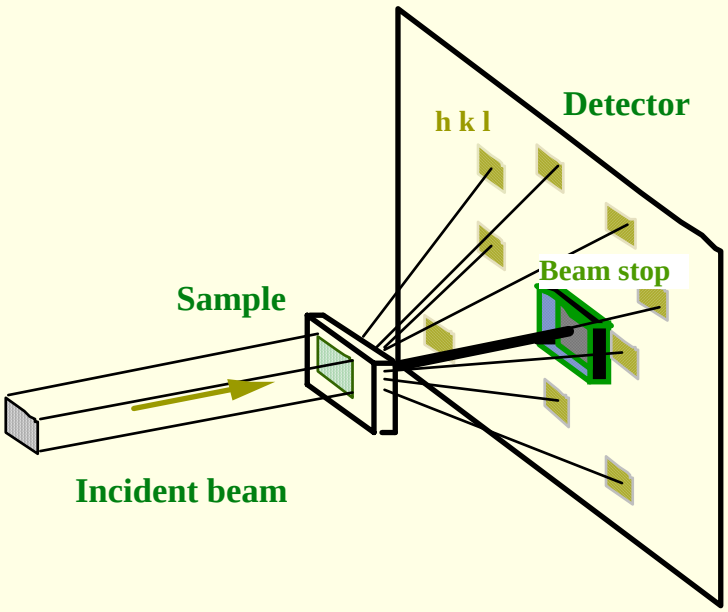

Double crystal topography

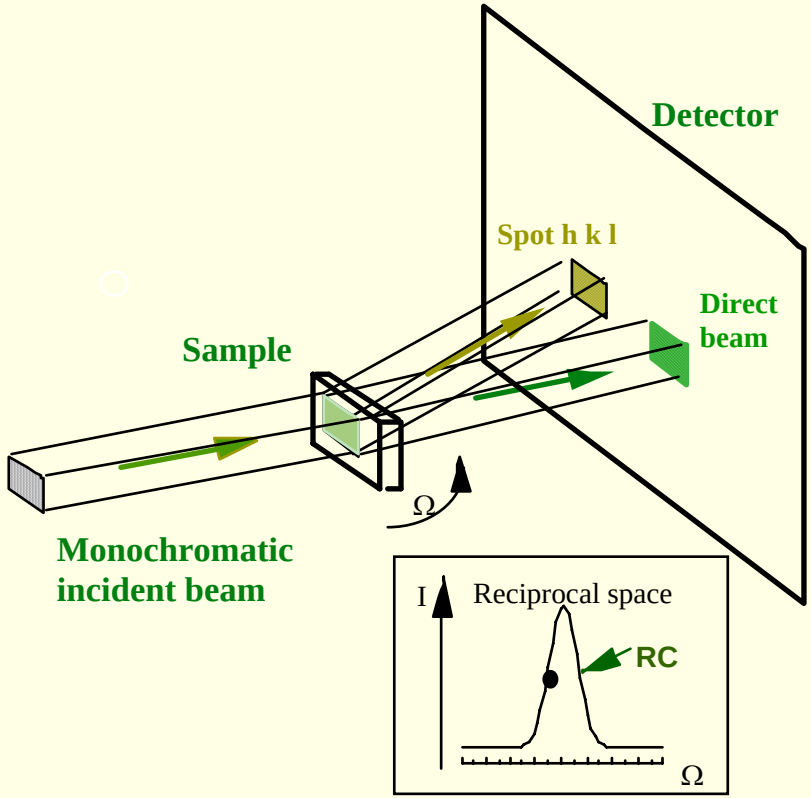

Simple application of the diffraction theory for perfect crystals

Well adapted for the interpretation of double crystal topographs

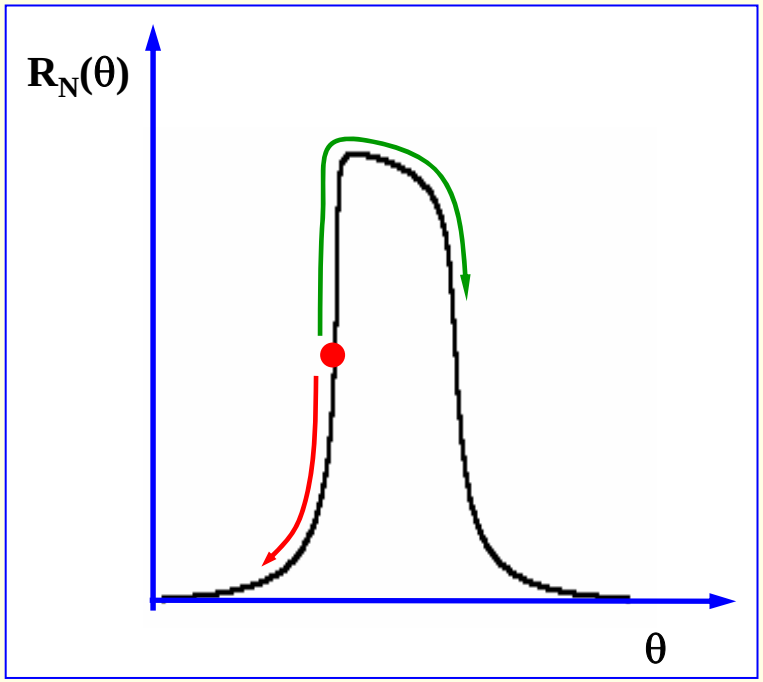

Local "shifting" of working point on the rocking curve

$$I_h = I_M \cdot R_N(\theta_A - \delta\theta)$$

If $\delta\theta << w_h^{\theta}$ **and** θ_A **on a linear part of the rocking curve**

$$I_h = M \cdot \delta\theta$$

« Weak beam » technique

Peak: when setting the crystal in the exact Bragg position the whole perfect crystal matrix participates to the diffraction: images of the defects can be complex

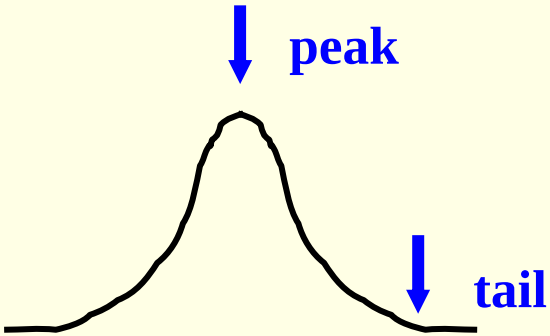

Tail: if the crystal is set on the tail of the rocking curve only distorted regions participate to the diffraction: defect images simpler and with better spatial resolution

h

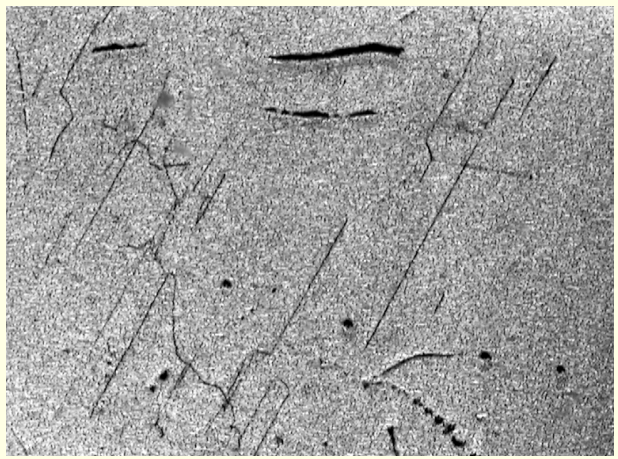

400µm

Diffraction imaging ("topography")
Frank-Read dislocation sources in SiC

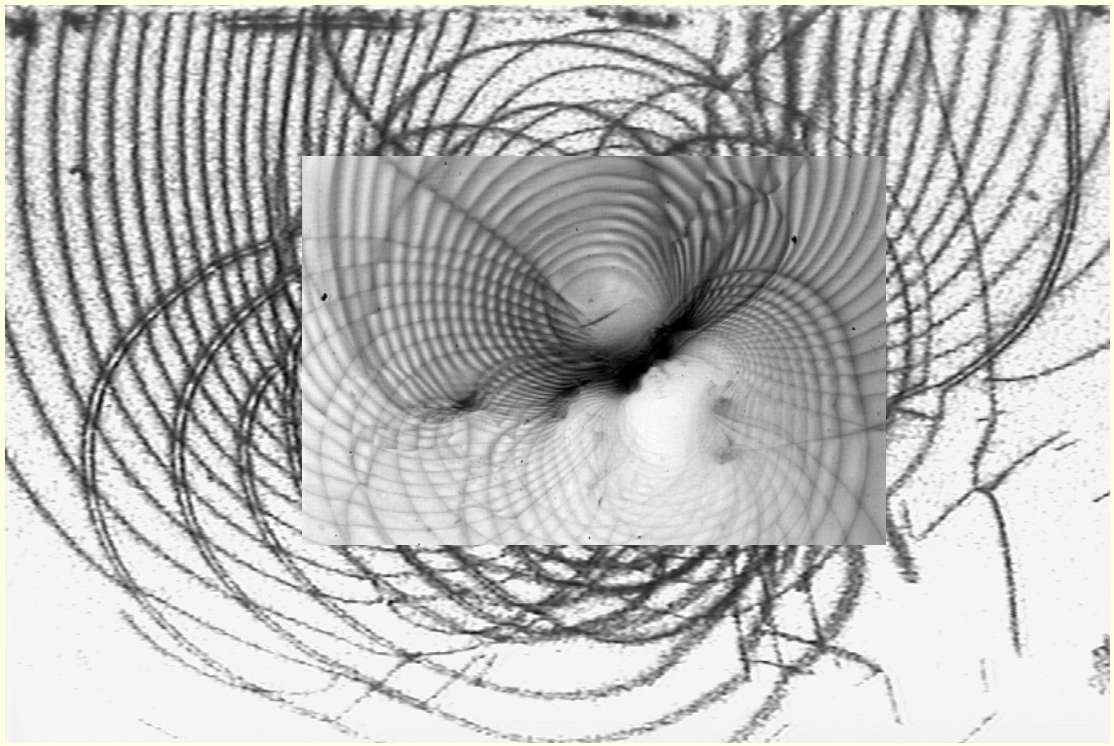

White beam topograph showing dislocations originating from several Frank-Read sources, not actually visible (distorted region)

« Weak beam » monochromatic topograph, which shows the location of the pinning centers (Frank-Read source)

Eetu PRIEUR, PhD Thesis, Helsinki 1997

Investigation of defects in bio-molecular crystals

Thaumatin

Space group P 4_1 2_1 2

a = 58.53Å, b = 58.53Å, c = 151.35Å, $\alpha = \beta = \gamma = 90°$

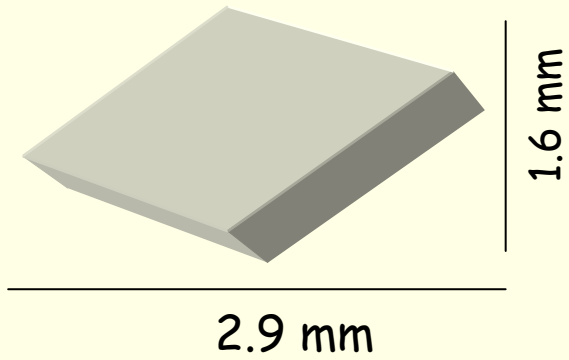

Dislocations

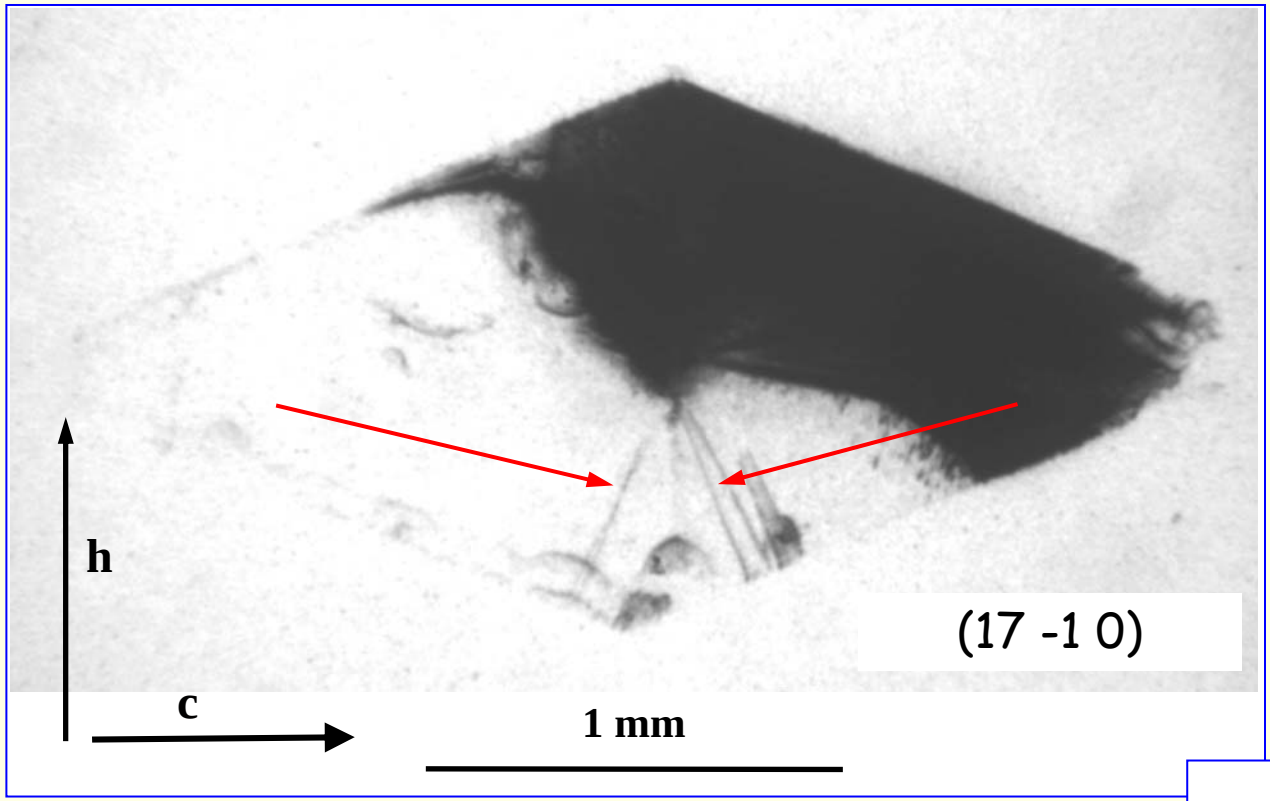

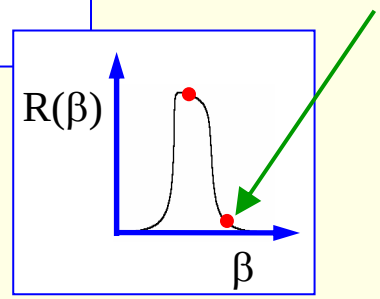

Only visible under weak beam conditions

Same features as any solution grown crystal

V. Stojanoff, B. Capelle, Y. Epelboin, F. Otalora, J. Härtwig

- Introduction
- Basic contrast mechanisms
- Diffraction topographic techniques (overview)
- **Simulations of topographic images**
- Combination of techniques (RCI, topo-tomography)
- Conclusion: new possibilities of modern synchrotrons for Bragg diffraction imaging

Simulation of X-ray topographs

X-ray topographs may be calculated:

- **local application of the diffraction theory for perfect crystals**
- **Kato theory (geometrical optical approximation, eikonal theory)**
- **Takagi theory (wave optical approximation)**

overview: J. Härtwig, *Hierarchy of dynamical theories of X-ray diffraction for deformed and perfect crystals*, J. Phys. D: Appl. Phys. **34**, A70-A77 (2001)

In most cases:

non-integrated images show more details
they are easier to simulate
they are easier to compare with experiment

Kato theory (geometrical optical approximation, eikonal theory)

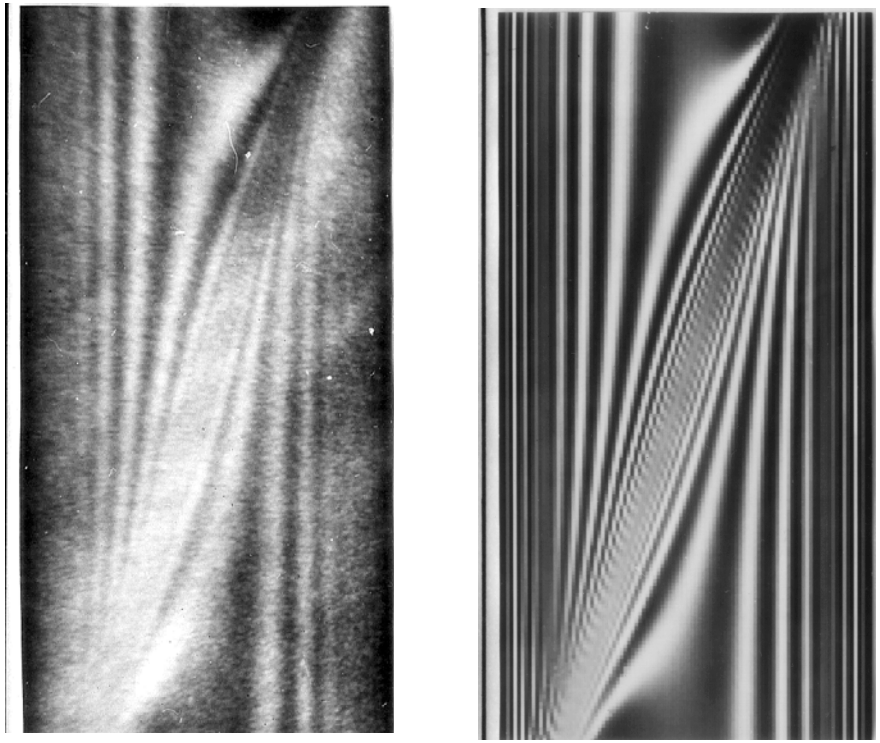

Comparison of a measured (left) and a calculated (right) **section topograph**, 565 μm silicon crystal with 150 nm silicon oxide film edges, symmetrical 422 reflection, 17.48 keV

Courtesy Jürgen Härtwig

- Introduction
- Basic contrast mechanisms
- Diffraction topographic techniques (overview)
- Simulations of topographic images
- **Combination of techniques**

  ⇨ Rocking Curve Imaging

  ⇨ topo-tomography
- Conclusion: new possibilities of modern synchrotrons for Bragg diffraction imaging

Rocking Curve Imaging

A tool to study the spatial distribution of strain, lattice tilts and dislocations on a micrometer scale

$GaPO_4$
009 reflection
E = 10 keV
1.4 μm pixel

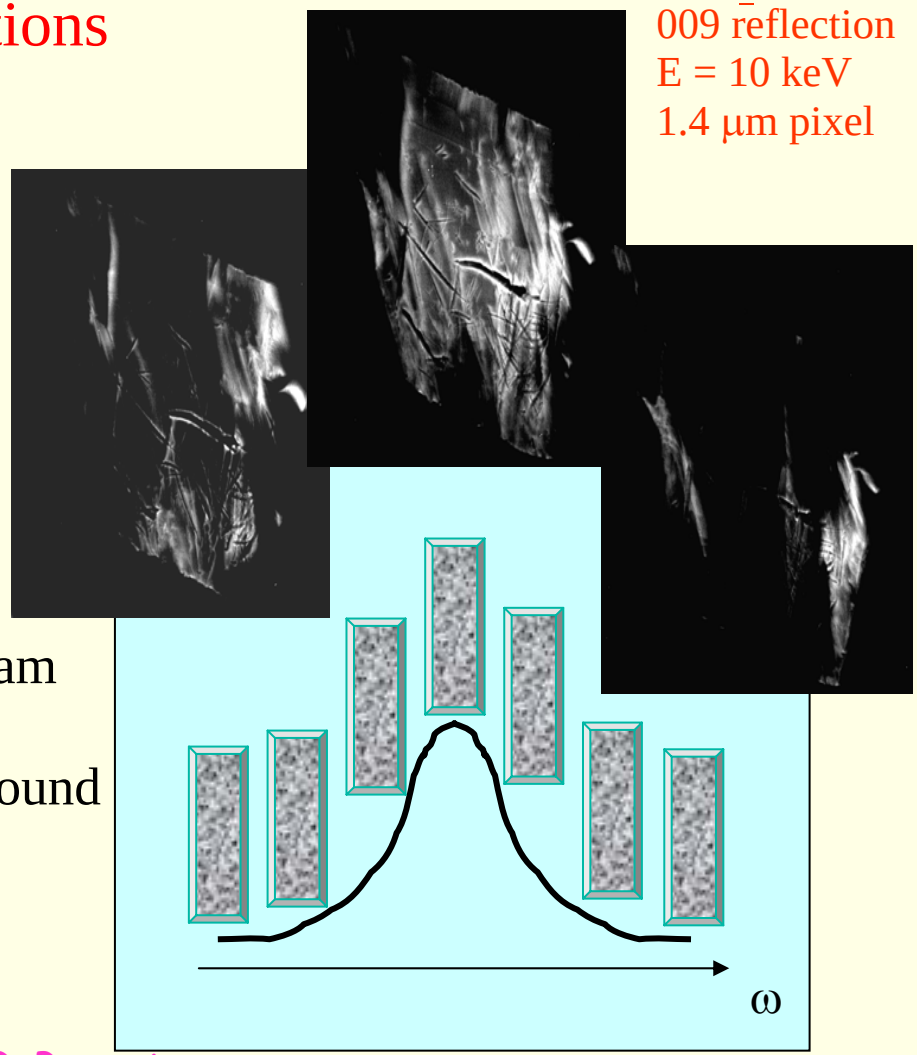

⇨ Diffractometry
(reciprocal space)

⇨ Monochromatic beam Topography
(real space)

MEASUREMENT
- wide, parallel, monochromatic X-ray beam
- 2D CCD detector
- record image at each angular position around Bragg peak

P. Mikulík, D. Lübbert, L. Helfen, T. Baumbach, P. Pernot

AREA DIFFRACTION (Rocking Curve Imaging)

DATA ANALYSIS

- 3D data blocks Intensity(x,y,ω)
- extract rocking curve for each pixel
- plot as 2D maps: spatially resolved distributions of FWHM, intensities, positions of maxima,…

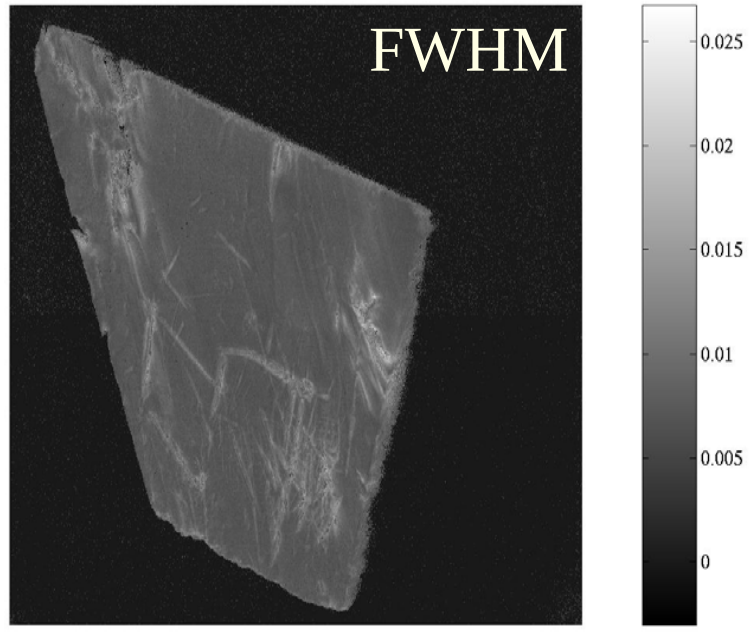

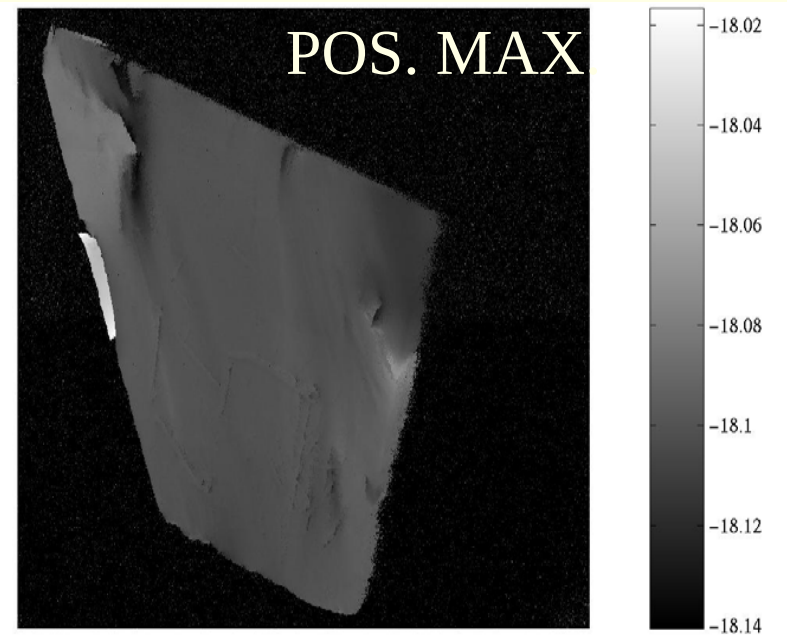

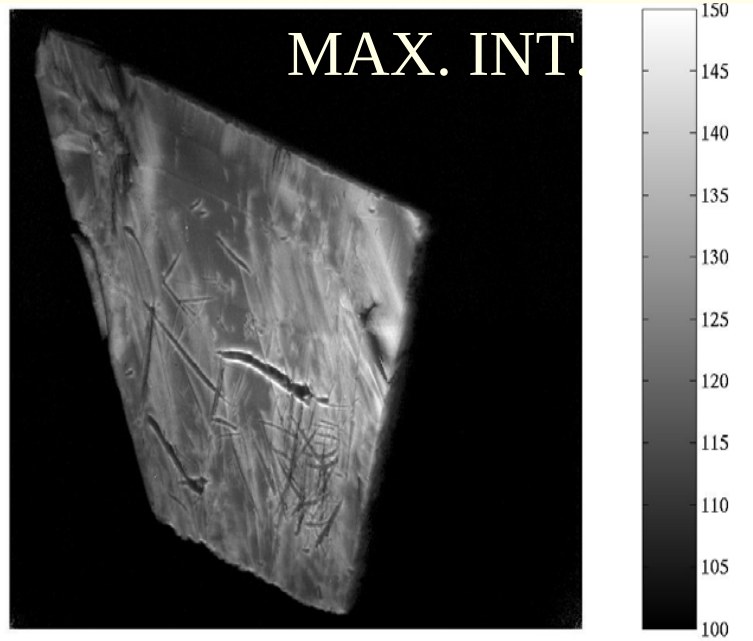

3D imaging of defects by topo-tomography

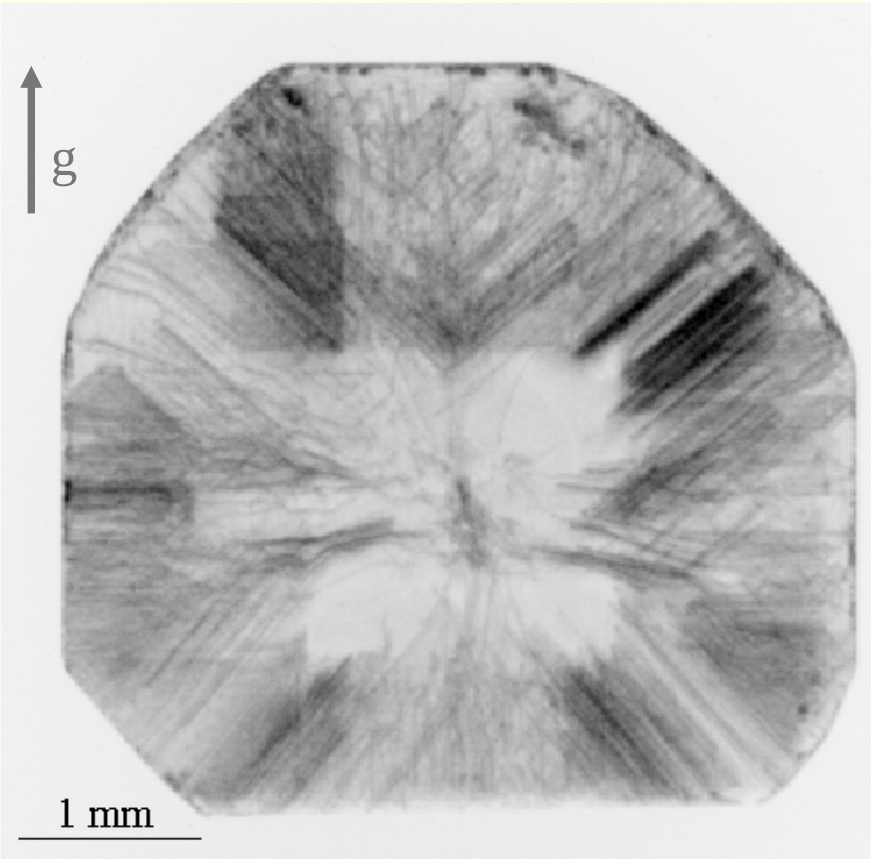

Integrated, monochromatic beam diffraction topograph of diamond single crystal

2D projection of 3D dislocation structure

In order to get 3D distribution:

- **Section topographs**
- **topographic stereopairs**
- **Topo-Tomography**

Turning around the diffraction vector

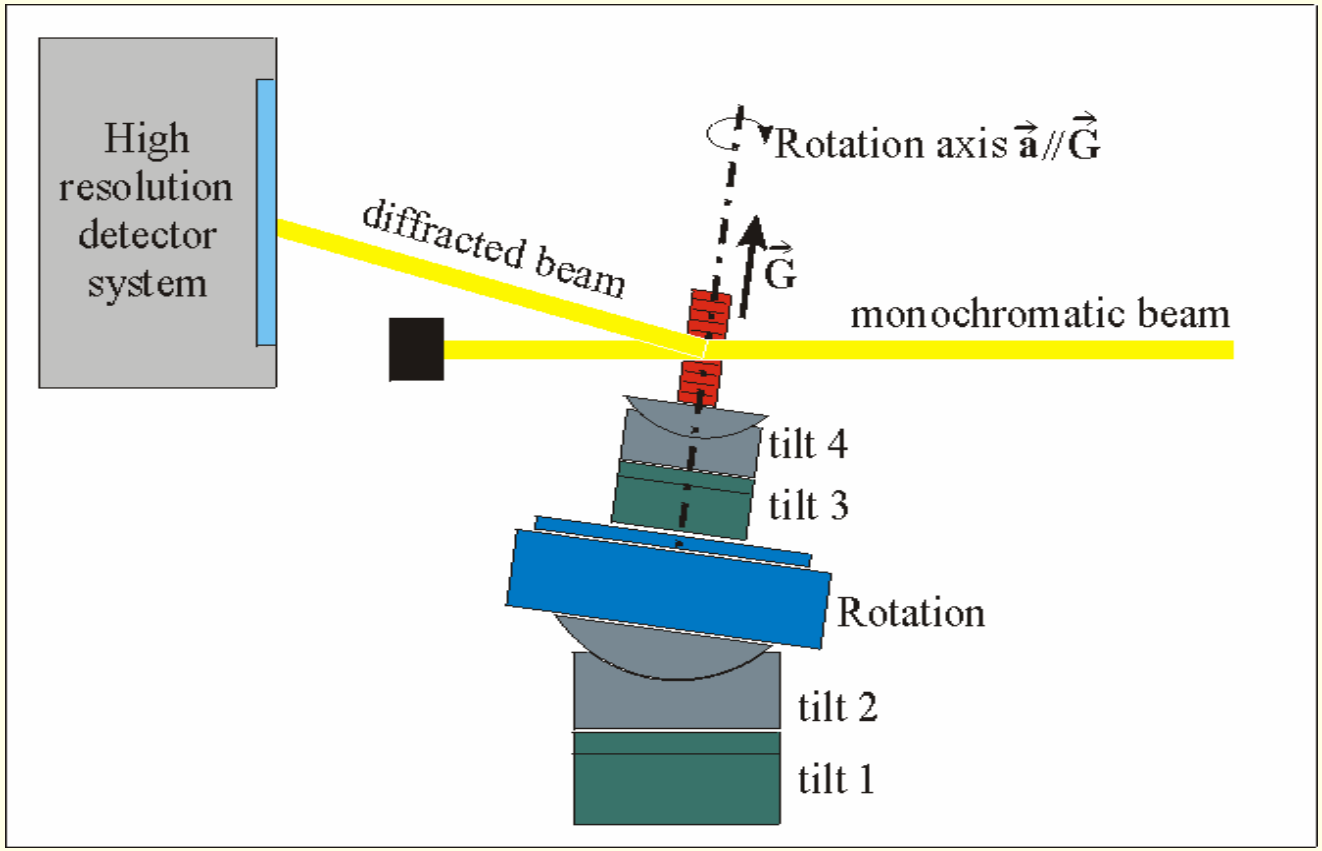

Topographs of a diamond sample

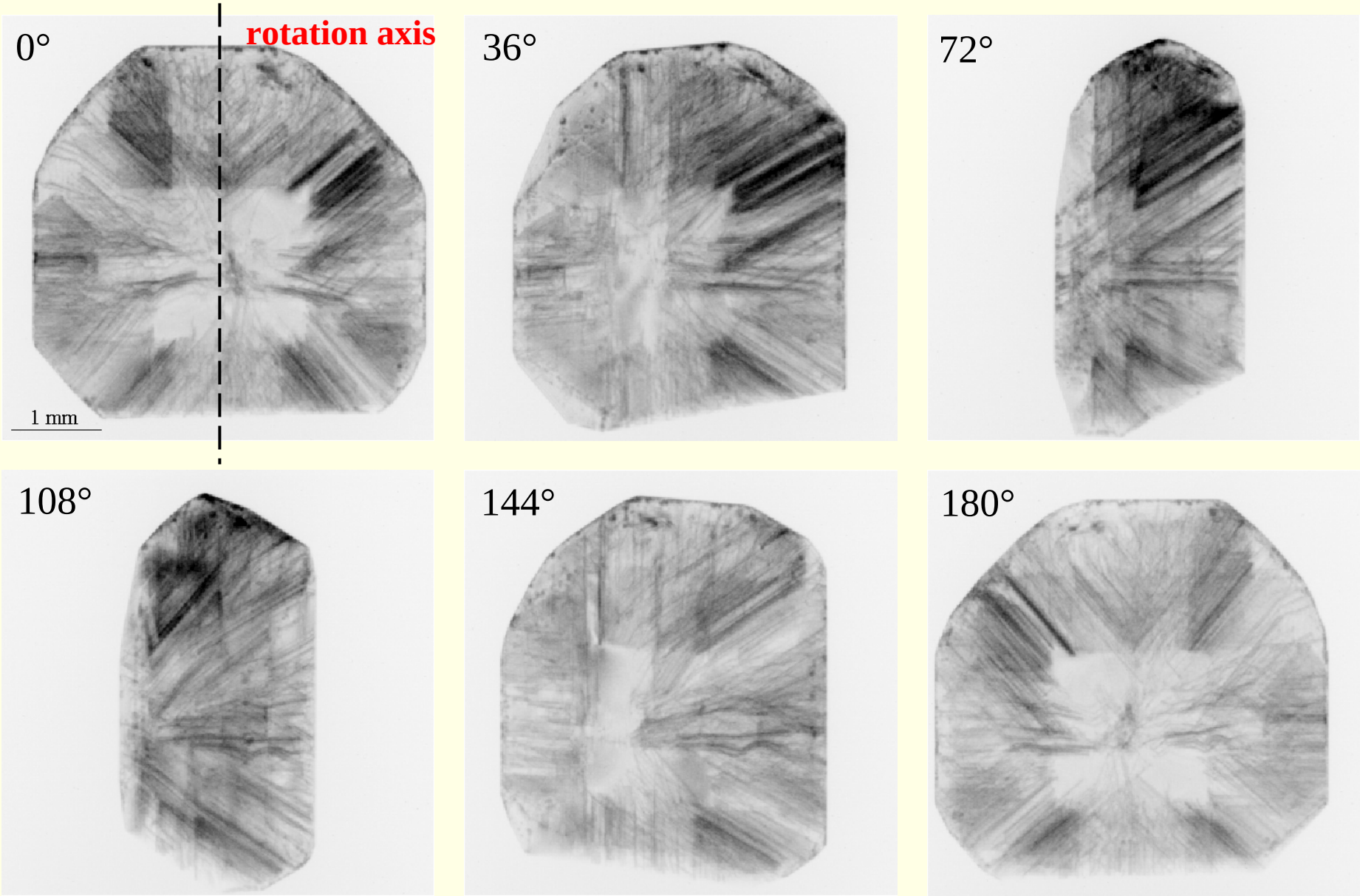

The Reconstruction

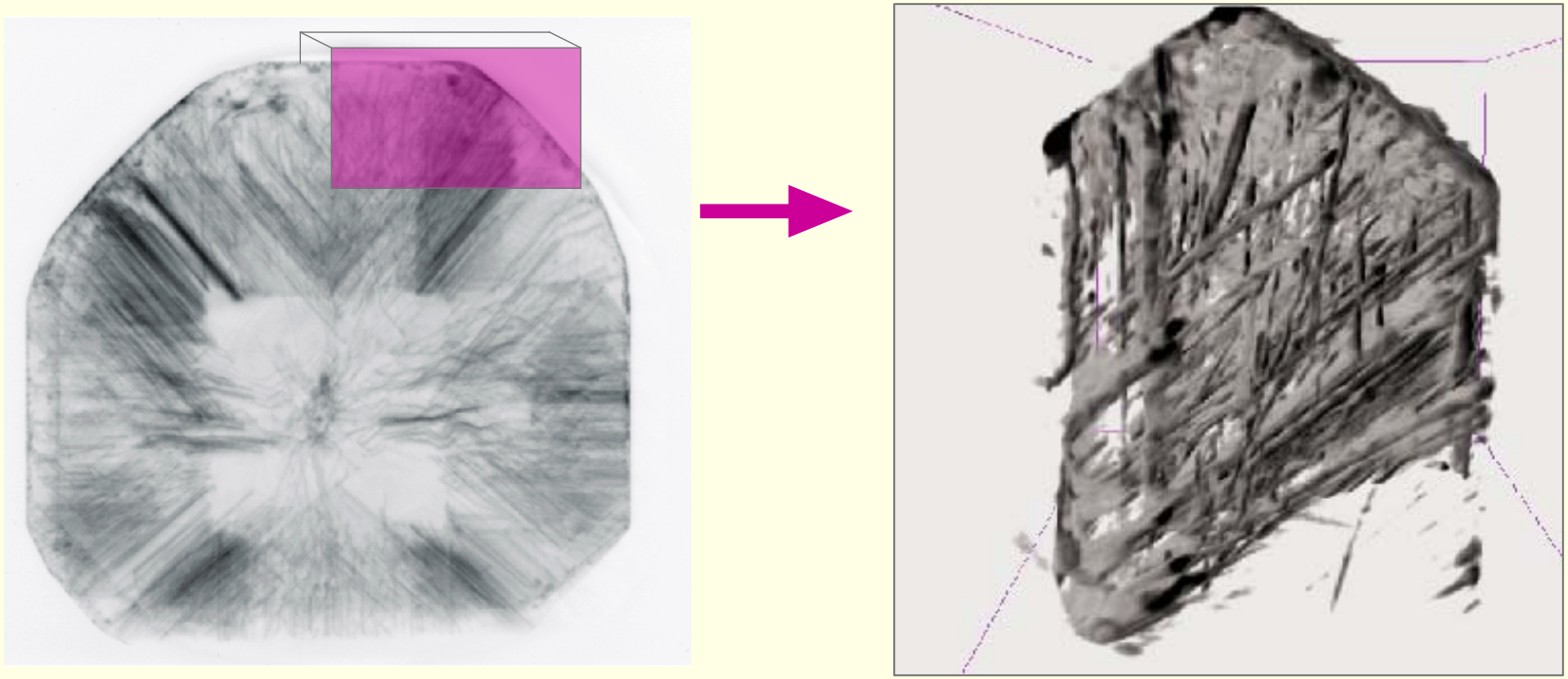

1 mm

W. Ludwig, P. Cloetens, J. Härtwig, J.Baruchel, B. Hamelin & P. Bastie,
J. Appl. Cryst. 34, 602-607 (2001)

- Introduction
- Basic contrast mechanisms
- Diffraction topographic techniques (overview)
- Simulations of topographic images
- Combination of techniques (RCI, Topo-tomography)
- **Bragg diffraction imaging at modern synchrotrons**

Enhanced or new possibilities for Bragg diffraction imaging at modern SR sources

Intensity: short exposure times (≥0.01s at ID19)

sample environment devices (crystal growth, high and low temperature, electrical and magnetic fields, mechanical traction, ..),

Wavelength range:

high energies accessible ⇨ bulky and strongly absorbing samples

Time structure:

stroboscopic diffraction imaging

Small angular source size ⇒ high geometrical resolution

sample to detector distance: new experimental parameter

Coherence: combination of Bragg and Fresnel diffraction

Conclusion on Bragg diffraction imaging

Bragg diffraction imaging (X-ray topography) remains a unique tool for the characterization of inhomogeneities (defects, domain boundaries, impurity distribution, waves,….) in crystals.

A lot of information can be extracted from an analysis that only takes into account orders of magnitude and uses a few simple criteria . Simulation of the images and comparison with the experiment allow further, quantitative, studies.

The actual interpretation of the diffraction images requires to know precisely the experimental conditions, because the contrast can vary dramatically (and even reverse) as a function of these conditions

Some literature

Tanner B.K. *X-ray diffraction topography*, Pergamon Press 1976

Characterization of crystal growth defects by X-ray methods, ed. by Tanner B.K. and Bowen D.K., Plenum press 1980

X-ray and neutron dynamical diffraction – Theory and applications ed. by Authier A., Lagomarsino S., Tanner B.K., Plenum Press 1996

Bowen D. K., Tanner B. K.: *High resolution X-ray diffractometry and topography*, Taylor & Francis Ltd 1998.

Authier A. *Dynamical theory of X-ray diffraction*, Oxford Univ. Press 2001

http://www.esrf.fr/exp_facilities/ID19/homepage/id19homepage.html

http://www.esrf.fr/exp_facilities/ID19/homepage/DiffTopo/X-raytopography.htm